

Heegaard Floer multicurves of double tangles

Claudius Zibrowius

ABSTRACT. We describe a simple formula for computing the Heegaard Floer multicurve invariant of double tangles from the Heegaard Floer multicurve invariant of knot complements. A comparison with a similar multicurve invariant for Conway tangles in the setting of Khovanov homology confirms that knot Floer homology and Khovanov homology behave very differently under satellite operations, echoing recent observations from [LZ22]. We also obtain a new characterisation of L-space knots in terms of Heegaard Floer A-link satellites. Along the way, we find the first example of a satellite knot whose knot Floer homology is thin.

1. Introduction

The double tangle T_K associated with an oriented knot $K \subset S^3$ is the Conway tangle obtained by cutting the knot K open to a tangle with two ends and adding another tangle strand parallel to the first, as illustrated in Figure 1. This family of Conway tangles plays a key role for understanding satellites of wrapping number 2: Any such satellite knot $P(K)$ can be written as

$$P(K) = T_K \cup T_P,$$

the union of the double tangle T_K associated with the companion knot K and a second Conway tangle T_P corresponding to the pattern P . This perspective allows us to investigate satellite formulae for any knot invariants that admit glueable generalisations to Conway tangles. For example, in joint work with Lukas Lewark, I recently applied this strategy to prove such satellite formulae for Rasmussen invariants [LZ22], using the multicurve tangle invariant generalising Bar-Natan homology [KWZ19].

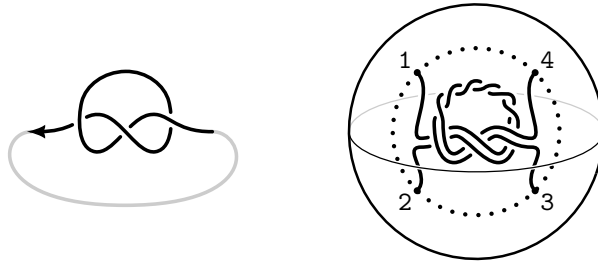


FIGURE 1. The double tangle (right) of the right-handed trefoil knot (left).

The focus of this paper lies on a similar multicurve invariant: the tangle invariant $\gamma_T := \text{HFT}(T)$ from Heegaard Floer theory [Zib20, Zib19b]. The main goal is to show that γ_{T_K} can be read off easily from yet another multicurve invariant, namely the Hanselman-Rasmussen-Watson multicurve $\gamma_K := \widehat{\text{HF}}(S^3 \setminus \mathring{\nu}(K))$ associated with the knot exterior [HRW16, HRW22]. Before explaining how this works, we briefly recall those features of the two multicurve invariants that are relevant to this story. The reader familiar with both invariants may skip straight to the statement of the Main Theorem (Page 5), which is illustrated in Figure 2.

1.1. A brief review of the multicurve invariant γ_K . The knot invariant γ_K is a multicurve, a finite set of free homotopy types of closed curves¹, on the one-punctured torus. This torus is naturally identified with the boundary of the knot exterior $S^3 \setminus \text{int}(\nu(K))$ and the puncture can be thought of as some basepoint z on said boundary.

To describe key properties of γ_K , we introduce some notation: Let μ_K denote a meridian of K and λ_K a longitude of K , both of which go through the basepoint z . We may assume without loss of generality that γ_K intersects the meridian μ_K and longitude λ_K transversally and minimally. Then by [HRW16, Example 6.8], the intersection points of γ_K with μ_K generate the knot Floer homology of K :

$$\widehat{\text{HFK}}(K) \cong \mathbb{F}_2 \langle \gamma_K \pitchfork \mu_K \rangle.$$

(We will work over the field \mathbb{F}_2 of two elements throughout this paper.) These intersection points cut the multicurve γ_K into *curve segments*, which can be characterized by how their ends approach μ_K and by how they intersect λ_K . To make this more precise, let \mathbb{R}^2 be the universal cover of the torus such that the integer lattice $\mathbb{Z}^2 \subset \mathbb{R}^2$ agrees with the preimage of the basepoint z . This is illustrated on the left of Figure 2. The preimage of μ_K under this covering map is equal to the union of the vertical lines $\tilde{\mu}_K := \mathbb{Z} \times \mathbb{R}$. Given a curve segment c of γ_K , consider a lift \tilde{c} to \mathbb{R}^2 . It starts and ends on some connected components $\tilde{\mu}_K^+$ and $\tilde{\mu}_K^-$ of $\tilde{\mu}_K$, respectively. We now say the curve segment c is of type

$$\begin{cases} \mathbf{u}_\ell & \text{if } \tilde{\mu}_K^+ = \tilde{\mu}_K^- \text{ and } \tilde{c} \text{ lies to the right of } \tilde{\mu}_K^\pm; \\ \mathbf{v}_\ell & \text{if } \tilde{\mu}_K^+ = \tilde{\mu}_K^- \text{ and } \tilde{c} \text{ lies to the left of } \tilde{\mu}_K^\pm; \\ \mathbf{d}_\ell & \text{if } \tilde{\mu}_K^+ \neq \tilde{\mu}_K^- \text{ (in which case } \tilde{c} \text{ lies between } \tilde{\mu}_K^+ \text{ and } \tilde{\mu}_K^- \text{)}. \end{cases}$$

In the first two cases, we call the subscript $\ell \in \mathbb{Z}$ the *length* of c ; in the third case, we call it the *slope* of c . In all three cases, $|\ell|$ equals the number of intersection points of c with λ_K . In the first two cases, this already determines the curve segments up to homotopy (relative to their endpoints), so we choose $\ell \geq 0$. In fact, $\ell > 0$ for any such curve segment, since we assume that γ_K intersects μ_K minimally. In the third case, we choose the sign of ℓ to be positive if and only if the slope of \tilde{c} is positive (after some homotopy relative endpoints). Clearly, the type of a curve segment c is independent of the choice of lift \tilde{c} and invariant under homotopy of c relative endpoints.

Remark 1.1. The multicurve invariant γ_K is equivalent to a version of knot Floer homology that takes the form of a chain complex over the polynomial ring

¹As part of the data of a multicurve, each curve is equipped with an orientation, a local system, and some grading data. Here, in the introduction, we will ignore any of these additional curve decorations.

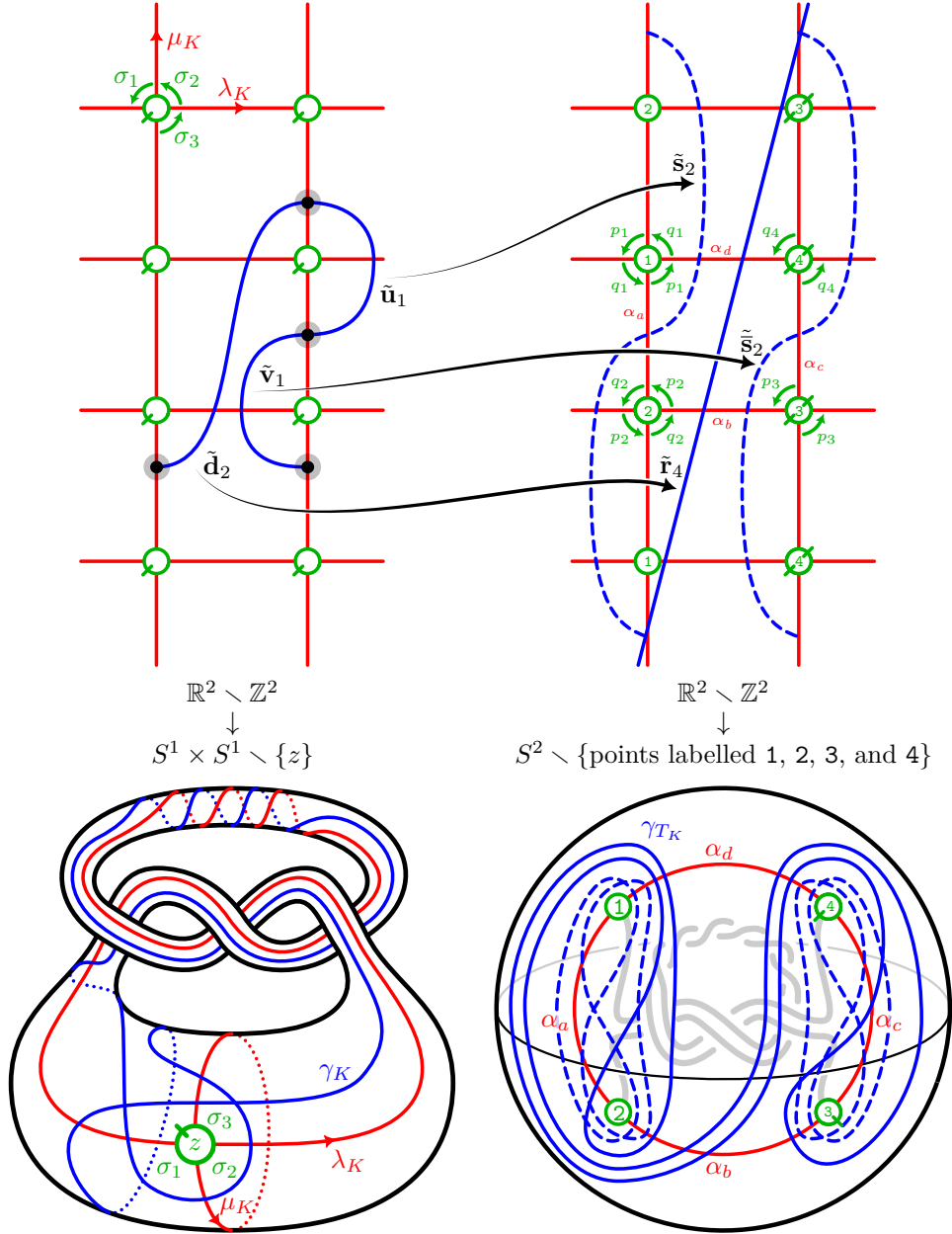


FIGURE 2. Executive summary of the Main Theorem (Page 5): To construct γ_{T_K} , first cut γ_K along the generators \bullet of $\overline{\text{HF}\overline{K}}(K)$ into curve segments. This always produces a single curve segment $\mathbf{d}_{2\tau(K)}$ of slope $2\tau(K)$ as well as some number of curve segments \mathbf{u}_ℓ and \mathbf{v}_ℓ that are right and left caps, respectively, of some length $\ell \in \mathbb{Z}^{>0}$. Then γ_{T_K} contains a rational component $\mathbf{r}_{4\tau(K)} := \mathbf{r}(4\tau(K))$ as well as a special component $\mathbf{s}_{2\ell} := \mathbf{s}_{2\ell}(\infty; 1, 2)$ and $\overline{\mathbf{s}}_{2\ell} := \mathbf{s}_{2\ell}(\infty; 3, 4)$ for every \mathbf{u}_ℓ and \mathbf{v}_ℓ in γ_K , respectively. Note: In all pictures except the bottom left, we are looking at the manifolds from the outside.

$\mathbb{F}_2[U, V]/(UV = 0)$; see for example [KWZ20, Theorem 2]. The curve segments \mathbf{u}_ℓ and \mathbf{v}_ℓ respectively correspond to components U^ℓ and V^ℓ of the differential in this chain complex.

The first part of the following structure theorem follows from [LOT18, Theorem 11.26]. The second part follows from the usual conjugation symmetry on knot Floer homology; see also [HRW22, Theorem 7].

THEOREM 1.2. *For any knot $K \subset S^3$, the multicurve γ_K contains exactly one curve segment $\mathbf{d}_{2\tau(K)}$, where $\tau(K)$ is the Ozsváth-Szabó concordance invariant, and every other curve segment is of type \mathbf{u}_ℓ or \mathbf{v}_ℓ for some $\ell \in \mathbb{Z}^{>0}$. Moreover, for any $\ell \in \mathbb{Z}^{>0}$,*

$$\#\{\text{curve segments in } \gamma_K \text{ of type } \mathbf{u}_\ell\} = \#\{\text{curve segments in } \gamma_K \text{ of type } \mathbf{v}_\ell\}.$$

1.2. A brief review of the multicurve invariant γ_T . The tangle invariant γ_T is also a multicurve; in this case, the multicurve lives on the four-punctured sphere which is naturally identified with the boundary of the three-dimensional ball containing the tangle minus the four tangle ends. Again, it is useful to consider the curves in a certain planar cover $\mathbb{R}^2 \setminus \mathbb{Z}^2$ of the four-punctured sphere, which is illustrated on the top right of Figure 2. The integer lattice corresponds to the four punctures of the sphere, labelled 1, 2, 3, and 4, the vertical lines $\mathbb{Z} \times \mathbb{R}$ are the preimage of the arcs connecting tangle ends (1 and 2) and (3 and 4) and similarly, the horizontal lines $\mathbb{R} \times \mathbb{Z}$ correspond to the arcs connecting (1 and 4) and (2 and 3).

The components of the multicurve γ_T are completely classified [Zib19b, Theorem 0.5]. We do not need the full classification here. We only describe those curves that show up as components of γ_{T_K} . First, an embedded simple closed curve in the four-punctured sphere is called a *rational curve of slope $k \in \mathbb{Z}$* , denoted by $\mathbf{r}(k)$ if it lifts to a straight line of slope k in the cover $\mathbb{R}^2 \setminus \mathbb{Z}^2$. Second, let $(\mathbf{i}, \mathbf{j}) = (1, 2)$ or $(3, 4)$. Consider an infinite straight line in $\mathbb{R}^2 \setminus \mathbb{Z}^2$ of slope ∞ going through some lattice points corresponding to the punctures \mathbf{i} and \mathbf{j} . The lattice points divide this line into intervals of equal length. For a fixed integer $\ell \in 2\mathbb{Z}^{>0}$, let us mark every ℓ th interval of the line. Then consider a small equivariant push-off of this line such that it intersects only the marked intervals and each of them exactly once. Finally, let $\mathbf{s}_\ell(\infty; \mathbf{i}, \mathbf{j})$ be the immersed, primitive curve in the four-punctured sphere that lifts to this push-off. We call $\mathbf{s}_\ell(\infty; \mathbf{i}, \mathbf{j})$ the *special curve of slope ∞ and length ℓ* through the punctures \mathbf{i} and \mathbf{j} . In this paper, we will use the following simplified notation:

$$\mathbf{r}_k := \mathbf{r}(k), \quad \mathbf{s}_\ell := \mathbf{s}_\ell(\infty; 1, 2), \quad \text{and} \quad \bar{\mathbf{s}}_\ell := \mathbf{s}_\ell(\infty; 3, 4).$$

The following structure theorem for γ_{T_K} is a special case of a general result for cap-trivial tangles, analogous in both statement and proof to [KWZ22a, Theorem 3.1].

THEOREM 1.3. *For any knot $K \subset S^3$, the multicurve γ_{T_K} contains exactly one curve segment \mathbf{r}_k , for some $k \in 2\mathbb{Z}$, and every other curve segment is of type \mathbf{s}_ℓ or $\bar{\mathbf{s}}_\ell$ for some $\ell \in 2\mathbb{Z}^{>0}$. Moreover, for any $\ell \in 2\mathbb{Z}^{>0}$,*

$$\#\{\text{components } \mathbf{s}_\ell \text{ of } \gamma_{T_K}\} = \#\{\text{components } \bar{\mathbf{s}}_\ell \text{ of } \gamma_{T_K}\}.$$

1.3. The Main Theorem. The similarity between the two structure theorems for γ_K and γ_{T_K} suggests a close relationship between the two invariants. And indeed, it is as simple as it can possibly be!

MAIN THEOREM. *The components of γ_{T_K} are in one-to-one correspondence with the curve segments obtained by splitting the curve γ_K along its intersection points with the meridian μ_K . More specifically, we have the following correspondence:*

$$\text{in } \gamma_K \left\{ \begin{array}{ccc} \mathbf{d}_{2\tau(K)} & \longleftrightarrow & \mathbf{r}_{4\tau(K)} \\ \mathbf{u}_\ell & \longleftrightarrow & \mathbf{s}_{2\ell} \\ \mathbf{v}_\ell & \longleftrightarrow & \bar{\mathbf{s}}_{2\ell} \end{array} \right\} \text{in } \gamma_{T_K}.$$

For a relatively bigraded version of this result, see Theorem 4.1.

Example 1.4. Figure 2 illustrates the Main Theorem for the right-handed trefoil knot $K = T_{2,3}$. The curve γ_K decomposes into three curve segments, namely \mathbf{d}_2 , \mathbf{u}_1 , and \mathbf{v}_1 . Hence, γ_{T_K} consists of three components: \mathbf{r}_4 , \mathbf{s}_2 , and $\bar{\mathbf{s}}_2$. Interestingly, as an ungraded curve, this agrees with the invariant of the quotient tangle $T_{K,h}$ of K under the unique strong inversion h on K [KWZ22a, Figure 4]. (The tangle $T_{K,h}$ is equal to the $(2, -3)$ -pretzel tangle, up to some number of twists, and its invariant γ_T was computed in [Zib20, Example 2.26].) However, as graded invariants, γ_{T_K} and $\gamma_{T_{K,h}}$ are distinct; see Example 4.2.

Remark 1.5. The multicurve invariants γ_K are very computable thanks to Szabó's computer program [OS17] and Hanselman's implementation of the arrow sliding algorithm [Han19]. Hanselman has compiled a list of the invariants for all knots up to 15 crossings, which is available on github along with the source code of his program. While there also exists software [Zib18] for computing the tangle invariant γ_T , it is neither as efficient nor as practical. Consequently, γ_T had so far only been known for very few tangles T other than the family of two-stranded pretzel tangles considered in [Zib20, Theorem 6.9]. The Main Theorem now provides an infinite family of new tangles for which the invariants are very easy to compute. The python script [Zib23] automates this computation, taking as input the multicurves γ_K in the format used in Hanselman's database [Han19].

1.4. A reformulation of the Main Theorem. Recall the following well-known structure theorem for $\text{HFK}^-(K)$, a version of knot Floer homology taking the form of a bigraded module over $\mathbb{F}_2[U]$; see for example [OSS15, Chapter 7].

THEOREM 1.6. *For any knot $K \subset S^3$, there exist integers $n \in \mathbb{Z}^{\geq 0}$ and $\ell_1, \dots, \ell_n \in \mathbb{Z}^{> 0}$ such that*

$$\text{HFK}^-(K) \cong \mathbb{F}_2[U] \oplus \bigoplus_{i=1}^n \mathbb{F}_2[U]/U^{\ell_i}.$$

The integers ℓ_1, \dots, ℓ_n are unique up to permutation.

The module $\text{HFK}^-(K)$ is generally not sufficient to determine γ_K . However, the curve segments of γ_K can be determined from $\text{HFK}^-(K)$. First, the Alexander grading of the generator of $\mathbb{F}_2[U]$ is equal to $-\tau(K)$, by definition. Second, using conjugation symmetry of knot Floer homology, one can show that for every U -torsion summand $\mathbb{F}_2[U]/U^{\ell_i}$ in $\text{HFK}^-(K)$, γ_K contains a pair of curve segments \mathbf{u}_{ℓ_i} and \mathbf{v}_{ℓ_i} . We therefore obtain the following reformulation of the Main Theorem.

THEOREM 1.7. *Given a knot $K \subset S^3$, let $n \in \mathbb{Z}^{\geq 0}$ and $\ell_1, \dots, \ell_n \in \mathbb{Z}^{> 0}$ be the integers determined by Theorem 1.6. Then*

$$\gamma_{T_K} = \mathbf{r}_{4\tau(K)} \cup \bigcup_{i=1}^n \mathbf{s}_{2\ell_i} \cup \bar{\mathbf{s}}_{2\ell_i}. \quad \square$$

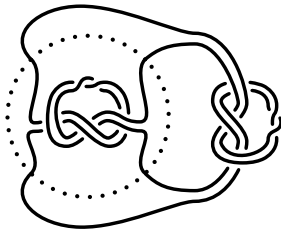


FIGURE 3. A satellite knot with thin knot Floer homology. The dotted circle indicates a Conway sphere splitting the knot into two tangles that agree with the double tangles of the left- and right-handed trefoil knots up to some twisting.

1.5. Consequences and questions: satellites, thinness, and A-links.

In 2021, Steve Boyer, Cameron Gordon, and Ying Hu showed that the Khovanov homology of any satellite knot is not thin, i.e. it is supported in more than one δ -grading [BGH21]. Up to now, the corresponding result for knot Floer homology was only known to be true for some specific patterns such as cables and the Mazur pattern [Dey19, PW21]. In fact, it is false in general:

THEOREM 1.8. *There exists a satellite knot $K \subset S^3$ for which $\widehat{\text{HFK}}(K)$ is thin.*

The knot in question is shown in Figure 3. At the time of writing, I do not know if this is the only such example.

Question 1.9. *Is this the only satellite knot with thin knot Floer homology?*

By applying thinness criteria for unions of Conway tangles from joint work with Artem Kotelskiy and Liam Watson [KWZ21] to the graded version of the Main Theorem (Theorem 4.1), we can give a partial answer to Question 1.9:

Proposition 1.10. *Let $K \subset S^3$ be a knot and P a pattern of wrapping number 2. Suppose K is neither the unknot nor a trefoil knot. Then $\widehat{\text{HFK}}(P(K))$ is not thin.*

Following [KWZ21], we call links whose knot Floer homology is supported in δ -gradings of the same parity *Heegaard Floer A-links*, or simply *A-links* for short. The set of A-links contains all alternating links, and more generally the set of thin links as a proper subset. This definition is inspired by the definition of L-spaces, which include all lens spaces [OS05a]. Recall that an L-space knot is a knot that admits any non-trivial L-space surgery. Similar to Proposition 1.10, we show:

Proposition 1.11. *Let $K \subset S^3$ be a knot and P a pattern of wrapping number 2. Suppose K is not an L-space knot. Then the satellite knot $P(K)$ is not an A-link.*

Given $p/q \in \mathbb{Q}P^1$, let $Q_{p/q}$ denote the rational tangle of slope p/q . We define the p/q -rational filling $T(p/q)$ of a Conway tangle T as the union $Q_{-p/q} \cup T$. If a rational filling of a tangle is an A-link, we call it a *rational A-link filling* [KWZ21]. Note that for any knot K , $T_K(\infty)$ is the unknot, so T_K always admits at least one rational A-link filling. This is analogous to the fact that there is at least one L-space surgery for any knot $K \subset S^3$, namely the ∞ -surgery. This analogy between rational A-link fillings and L-space surgeries goes much further:

THEOREM 1.12. *A knot $K \subset S^3$ admits a non-trivial L-space surgery if and only if its double tangle T_K admits a non-trivial rational A-link filling.*

We compare the relevant filling slopes in Theorem 5.3.

1.6. Consequences and questions: growth under cabling. An open question about the Heegaard Floer tangle invariant γ_T (in fact, any of the multicurve invariants now existing in low-dimensional topology) is how to interpret the number of their components. Thanks to the Main Theorem, double tangles $T = T_K$ are the first family of tangles for which we can give a fairly satisfying answer:

Corollary 1.13. *For any knot $K \subset S^3$,*

$$\#\{\text{connected components in } \gamma_{T_K}\} = \dim \widehat{\text{HFK}}(K). \quad \square$$

This has the following consequence for the growth of knot Floer homology of cable knots $C_{2,2t+1}(K)$ of winding number 2.

Proposition 1.14. *Given a knot $K \subset S^3$, let $d = \dim \widehat{\text{HFK}}(K)$ and let $\bar{\ell}$ be the average torsion order of $\text{HFK}^-(K)$, i.e. the arithmetic mean of the integers ℓ_i in Theorems 1.6 and 1.7. Then for any $t \in \mathbb{Z}$,*

$$\dim \widehat{\text{HFK}}(C_{2,2t+1}(K)) = 2(d-1)\bar{\ell} + |2t+1 - 4\tau(K)|.$$

In particular,

$$2(d-1)\ell_{\max} + |2t+1 - 4\tau(K)| \geq \dim \widehat{\text{HFK}}(C_{2,2t+1}(K)) \geq 2d-1,$$

where ℓ_{\max} is the maximum torsion order of $\text{HFK}^-(K)$.

The average torsion order $\bar{\ell}$ may be arbitrarily large, as demonstrated by the fact that for any positive integer n , the value of $\bar{\ell}$ for the torus knot $K = T_{n,n+1}$ is equal to $\frac{n}{2}$. Usually, however, $\bar{\ell}$ is very close to 1. In fact, among all the knots up to 15 crossings, the average value of $\bar{\ell}$ is about 1.00077 [Han19, Zib23]. Its maximum value is 2 among those knots (realized by $13n_{4639} = C_{2,5}(T_{2,3})$ and $15n_{41185} = T_{4,5}$). So one might interpret Proposition 1.14 as saying that $\dim \widehat{\text{HFK}}(C_{2,2t+1}(K))$ depends approximately linearly on $d = \dim \widehat{\text{HFK}}(K)$. This is in stark contrast to the non-linear behaviour of reduced Khovanov homology:

Proposition 1.15. *Given a knot $K \subset S^3$, let $d = \dim \widetilde{\text{Kh}}(K)$. Then for any $t \in \mathbb{Z}$,*

$$\dim \widetilde{\text{Kh}}(C_{2,2t+1}(K)) \geq 2d^2 - 2 + |2t+1 - 2\vartheta_2(K)|,$$

where $\vartheta_2(K)$ is the concordance homomorphism introduced in [LZ22].

This result is basically an application of the link splitting spectral sequence in Khovanov homology of Batson and Seed [BS15]. Computations suggest that this behaviour extends to the number of components in the reduced Khovanov multicurve invariant $\widetilde{\text{Kh}}(T_K)$ of double tangles [KWZ19]. We will explore the following conjecture in upcoming work.

Conjecture 1.16. *For any knot $K \subset S^3$, the number of special components in $\widetilde{\text{Kh}}(T_K)$ is bigger or equal to $\frac{1}{2}(d^2 - 1)$, where d is the dimension of the reduced Khovanov homology of K . For two-bridge knots, this bound is sharp.*

On a perhaps more speculative note, the decomposition of the multicurve γ_K into curve segments might also be relevant in relation to the Khovanov multicurve invariant $\widetilde{\text{Kh}}(T)$, specifically in view of the spectral sequence [OS05b].

Observation 1.17. *For all strongly invertible knots (K, h) with up to 9 crossings, the number of special components of $\widetilde{\text{Kh}}(T_{K, h})$ is bounded below by the number of curve segments \mathbf{u}_ℓ in γ_K . In fact we have equality for all such knots, except 9_{46} , the only such knot with two strong inversions h_1 and h_2 for which the (ungraded) Khovanov multicurve invariants do not agree [KWZ22a].*

It would be interesting to compute the Heegaard Floer multicurve invariant γ_T of quotient tangles of strongly invertible knots to see if the identity of the tangle invariants in Example 1.4 is part of a general pattern.

Outline of the paper. In Section 2, we recall the construction of the multicurve invariants γ_K and γ_{T_K} and we discuss gradings in both settings. In Section 3, we compute the bordered sutured type AD bimodule that turns the type D structure corresponding to the knot complement into the type D structure for the corresponding double tangle. In Section 4, we interpret the action of this bimodule in terms of multicurves, proving the Main Theorem. In Sections 5 and 6, we prove the results from Subsections 1.5 and 1.6, respectively. Throughout this paper, we will assume familiarity with bordered and bordered sutured Heegaard Floer homology [LOT18, Zar11] as well as basic techniques for modifying chain complexes over categories within their homotopy class; see for instance [Zib20, Section 1].

Acknowledgements. This paper was motivated by joint work with Lukas Lewark [LZ22]. I am very grateful to him for his generous support over the past two years and for giving me the freedom to pursue my own research as his postdoc. I would also like to thank Jake Rasmussen, Liam Watson, and Paul Wedrich for helpful conversations about the behaviour of knot Floer and Khovanov homology under cabling. Finally, I thank Jen Hom and Biji Wong for their helpful questions and comments after a talk I gave about this work at the low-dimensional topology workshop in Budapest in March 2023, which motivated me to explore some further applications of the Main Theorem and which allowed me to improve the exposition. During the course of this work, I was funded through the Emmy Noether Programme of the DFG, project number 412851057, and an individual research grant of the DFG, project number 505125645.

2. Review and conventions

2.1. A more detailed review of the multicurve invariant γ_K . The invariant γ_K is a topological interpretation of a certain bordered Heegaard Floer invariant. We start with a description of the latter and then explain how it is related to γ_K .

The bordered structure on the knot exterior. The exterior $X_K := S^3 \setminus \text{int}(\nu(K))$ of an oriented knot $K \subset S^3$ is a three-manifold with torus boundary. On this torus ∂X_T , we fix two simple closed curves, namely a meridian μ_K and a longitude λ_K of K , that intersect in a single point z , which we may regard as a basepoint on ∂X_K . The longitude is a push-off of K , inheriting its orientation. The orientation of the meridian is determined by the right-hand rule. This decoration of ∂X_K can be turned into a bordered structure as follows: Around z , we add a small circle that intersects μ_K and λ_K minimally and which one may think of as a suture. The restriction of μ_K to the complement of the interior of the disc bounded by the suture is an oriented arc, which we denote by \mathbf{a}_\bullet . Similarly, λ_K gives rise to an oriented arc \mathbf{a}_\circ with ends on the suture. We now add a basepoint to the suture; by convention,

it sits immediately between the endpoints of \mathbf{a}_\bullet and \mathbf{a}_\circ . This is illustrated at the bottom left of Figure 2. The arc diagram \mathcal{Z}_α consisting of the suture together with this basepoint and the arcs \mathbf{a}_\bullet and \mathbf{a}_\circ embedded on ∂X_K is a bordered structure for X_K . Now the algebraic invariant corresponding to the multicurve γ_K is the type D structure $\widehat{\text{CFD}}(X_K)^\mathcal{A}$ associated with X_K equipped with this bordered structure. For the construction of $\widehat{\text{CFD}}(X_K)^\mathcal{A}$, we refer the reader to [LOT18]; we only recall its formal properties, following [LOT18, Section 11].

The torus algebra. We define $\widehat{\text{CFD}}(X_K)^\mathcal{A}$ as a graded right type D structure over the bordered algebra $\mathcal{A}(\mathcal{Z}_\alpha, 1)$ with one moving strand, which we identify with the quiver algebra

$$\mathcal{A} := \mathbb{F}_2 \left[\begin{array}{ccc} & \xrightarrow{\sigma_1} & \circ \\ \bullet & \xrightarrow{\sigma_2} & \circ \\ & \xrightarrow{\sigma_3} & \circ \end{array} \right] / \left(\sigma_1 \sigma_2 = 0 = \sigma_2 \sigma_3 \right).$$

We denote the idempotents in \mathcal{A} by ι_\bullet and ι_\circ , respectively. We also write $\sigma_{12} := \sigma_2 \sigma_1$, $\sigma_{23} := \sigma_3 \sigma_2$, and $\sigma_{123} := \sigma_3 \sigma_2 \sigma_1$. The algebra \mathcal{A} is graded by some non-commutative groups, which we will discuss later. For the moment, we will also ignore the grading on $\widehat{\text{CFD}}(X_K)$, which takes values in the set of certain cosets of these groups.

Remark 2.1. We have renamed the elements of the algebra \mathcal{A} , usually denoted by the letter ρ instead of σ , to avoid confusion with the elements p_i of the algebra \mathcal{B} that we will introduce below. More importantly, the invariant of X_K was originally defined as a *left* type D structure ${}^{\mathcal{A}^{op}}\widehat{\text{CFD}}(X_K)$ over the opposite algebra \mathcal{A}^{op} of \mathcal{A} [LOT18, HRW16]. Our conventions have the advantage that the multiplication in the torus algebra \mathcal{A} is read from right to left, like morphisms in a category. In fact, we usually consider \mathcal{A} as a category with two objects and we regard type D structures simply as chain complexes over this category; see [Zib20, Section 1].

Example 2.2. For the unknot U and the right-handed trefoil knot $T_{2,3}$, we have

$$\widehat{\text{CFD}}(X_U)^\mathcal{A} \cong \left[\bullet \curvearrowright \sigma_{12} \right] \quad \text{and} \quad \widehat{\text{CFD}}(X_{T_{2,3}})^\mathcal{A} \cong \left[\begin{array}{ccc} \bullet & \xrightarrow{\sigma_2} \circ & \xleftarrow{\sigma_3} \bullet \\ \sigma_1 \downarrow & & \downarrow \sigma_1 \\ \circ & & \circ \\ \sigma_{23} \swarrow & & \nwarrow \sigma_{123} \\ & \circ & \xleftarrow{\sigma_3} \bullet \end{array} \right].$$

These labelled graphs should be understood as follows: Each vertex represents a generator/basis element of the underlying chain module of the chain complex. Each arrow corresponds to a non-zero entry of the square matrix representing the differential when written with respect to the chosen basis. The entries of this square matrix are the elements of \mathcal{A} specified by the arrow labels.

The complexes in the above example have the remarkable property that each of them arises from an immersed curve on a one-punctured torus via the following general construction.

From curves to chain complexes. Let Σ be a one-punctured torus $S^1 \times S^1 \setminus \text{int}(D^2)$, decorated by two arcs \mathbf{a}_\bullet and \mathbf{a}_\circ , just like ∂X_K above. In fact, if K is given, we identify Σ with ∂X_K minus a disc bounded by the suture. Let γ be a collection of non-contractible and primitive immersed curves $S^1 \looparrowright \Sigma$ that intersects \mathbf{a}_\bullet and \mathbf{a}_\circ minimally and transversely. For the second complex in the above example, γ is

the blue curve γ_K on the bottom left of Figure 2; for the first complex, the curve agrees with the longitude of U . Each point in $\gamma \cap \mathbf{a}_\bullet$ corresponds to a generator in idempotent ι_\bullet , and similarly, each point in $\gamma \cap \mathbf{a}_\circ$ corresponds to a generator in idempotent ι_\circ . The arcs cut γ into curve segments, each of which corresponds to an arrow (= a component of the differential) in the complex, connecting the two generators for the ends of the curve segment. To determine the direction and labels of these arrows, we first need to fix a labelling of some paths on $\partial\Sigma$. Up to reparametrization, there are four elementary paths on $\partial\Sigma$, i.e. paths that start and end on $\partial(\mathbf{a}_\bullet \cup \mathbf{a}_\circ)$, that follow the induced orientation on $\partial\Sigma$, and whose interiors avoid $\partial(\mathbf{a}_\bullet \cup \mathbf{a}_\circ)$. By convention, we label three of these consecutive paths by σ_1 , σ_2 , and σ_3 as shown in Figure 2. Now, every curve segment of γ is homotopic (relative to $\mathbf{a}_\bullet \cup \mathbf{a}_\circ$) to either σ_1 , σ_2 , or σ_3 , or one of their compositions, and each curve segment inherits its orientation and label from this path on $\partial\Sigma$.

Chain complexes over \mathcal{A} that (up to chain homotopy) arise from this construction and that can be appropriately graded (see below) are called *loop-type* [HW15]. However, as we will see in a moment, not every chain complex is loop-type.

Curves with local systems. Let γ be a curve in the torus as above, but consisting of a single component only. Also, let n be some positive integer and let (C, d) be a chain complex that arises from γ using the previous construction. Then $(C \otimes \mathbb{F}_2^n, d \otimes \text{id}_{\mathbb{F}_2^n})$ is also a well-defined chain complex. We now modify its differential as follows: First, we fix an orientation of γ . Next, let x and y be two basis elements for (C, d) such that the differential d has a component a from x to y . In the new chain complex, this component corresponds to a component $a \otimes \text{id}_{\mathbb{F}_2^n}$. We now change this component to $a \otimes X$ or $a \otimes X^{-1}$, depending on certain orientation conventions, where $X \in \text{GL}_n(\mathbb{F}_2)$. One can show that the chain homotopy type of the resulting chain complex is independent of the choice of basis elements x and y (see the remarks at the end of the proof of [HRW16, Theorem 1.5]). We can therefore denote this chain complex simply by $C(\gamma, X)$. We call X the local system of the oriented curve γ . For $n > 0$, the local systems $X = \text{id}_{\mathbb{F}_2^n}$ are called trivial.

Definition 2.3. Given a collection $\{(\gamma_i, X_i)\}_i$ of curves with local systems, we define the associated chain complex as the direct sum of the chain complexes $C(\gamma_i, X_i)$. Two collections $\{(\gamma_i, X_i)\}_i$ and $\{(\gamma'_j, X'_j)\}_j$ of curves with local systems are considered equal (and can be shown to induce the same chain complexes up to homotopy) if for any curve γ , the matrices

$$\bigoplus_{\gamma=\gamma_i} X_i \oplus \bigoplus_{-\gamma=\gamma_i} X_i^{-1} \quad \text{and} \quad \bigoplus_{\gamma=\gamma'_j} X'_j \oplus \bigoplus_{-\gamma=\gamma'_j} X'^{-1}_j$$

are similar. Here, $-\gamma$ denotes the curve γ with the opposite orientation and two oriented immersed curves are considered equal if they are homotopic.

Classification result. Chain complexes arising from curves with local systems are *extendable*, which is a certain algebraic property that is immaterial to our discussion. We only need to know the following result of Hanselman-Rasmussen-Watson [HRW16, Theorem 1.4], which is essentially due to Lipshitz-Ozsváth-Thurston [LOT18, Chapter 11].

THEOREM 2.4. *For every knot $K \subset S^3$, $\widehat{\text{CFD}}(X_K)^{\mathcal{A}}$ is extendable.*

This is relevant in the context of the following classification result of Hanselman-Rasmussen-Watson [HRW16, Theorem 1.5].

THEOREM 2.5. *Every extendable graded chain complex over \mathcal{A} is chain homotopic to a chain complex corresponding to a collection of curves with (possibly trivial) local systems. This collection of curves with local systems is unique up to the equivalence from Definition 2.3.*

Combining these two results, we can now finally define:

Definition 2.6. For any knot $K \subset S^3$, let γ_K denote the collection of immersed curves with local systems on ∂X_K corresponding to $\widehat{\text{CFD}}(X_K)^{\mathcal{A}}$.

Definition 2.7. Given a collection $\gamma = \{(\gamma_i, X_i)\}_i$ of curves with local systems, we define the curve segments $S_{\infty}(\gamma)$ as the set of (graded) type D structures obtained as follows: Let D_i be the type D structure corresponding to the curve γ_i . Split D_i along each generator in idempotent \bullet like so:

$$(\cdots \longleftrightarrow \bullet \longleftrightarrow \cdots) \text{ becomes } (\cdots \longleftrightarrow \bullet) \quad (\bullet \longleftrightarrow \cdots).$$

Let $\{D_{i,j}\}_j$ be the connected components of the resulting type D structure. We now define $S_{\infty}(\gamma)$ as the set of type D structures that for each pair (i, j) contains $\dim X_i$ copies of $D_{i,j}$.

Clearly, the elements of $S_{\infty}(\gamma)$ correspond to the curve segments \mathbf{u}_{ℓ} , \mathbf{v}_{ℓ} , and \mathbf{d}_{ℓ} from the introduction.

2.2. A more detailed review of the multicurve invariant $\gamma_{\mathcal{T}}$. Like the multicurve γ_K , the tangle invariant γ_{T_K} is a topological interpretation of a certain bordered (in fact: bordered sutured) Heegaard Floer invariant. But before describing any of this, we fix some conventions regarding Conway tangles, largely following [Zib20, Section 2.1] and [LZ22, Section 2.1].

Conway tangles. An *oriented Conway tangle* T is a proper embedding of two intervals into a three-dimensional ball B^3 , considered up to ambient isotopy. A *framing* of B^3 is a circle Φ on $S^2 = \partial B^3$ together with a choice of four points on this circle that are consecutively labelled 1, 2, 3, and 4. We consecutively label the four arcs $\Phi \setminus \{1, 2, 3, 4\}$ by α_a , α_b , α_c , and α_d , starting with the arc between 1 and 2. A *framed oriented Conway tangle* is a Conway tangle together with a choice of framing of B^3 which identifies the endpoints of the two intervals with the four points 1, 2, 3, and 4. We consider framed tangles up to ambient isotopy which identifies the framings. In the following, we will refer to framed, oriented Conway tangles simply as *Conway tangles*.

The *double tangle* T_K of an oriented knot K is the Conway tangle that is defined as follows: Let L be the oriented link obtained as the union of K with one of its zero-framed longitudes, regarded as a small push-off of K . Then L bounds an embedded (unoriented) annulus in S^3 , namely the image of a suitably chosen homotopy between K and the longitude. Now choose a small open three-ball b which intersects this annulus in a trivially embedded band. Then T_K is defined as the intersection of L with the complement B^3 of b . We choose the framing of T_K that is (up to homotopy and up to interchanging the two components of T_K) uniquely characterized by the following properties:

- (1) the intersection of ∂B^3 with the band is equal to the arcs α_a and α_c ,
- (2) in the closure of the three-ball b , the restriction of L and the arcs α_b and α_d cobound two discs (ensuring that the linking number of the two strands in T_K vanishes), and

(3) the orientation of the tangle points out of B^3 at the tangle ends 1 and 2. In particular, it follows that

(4) the tangle connects the tangle end 1 with 4 and 2 with 3.

A Conway tangle satisfying (4) is said to have *horizontal connectivity*. We implicitly assume from now that all Conway tangles that we consider satisfy (3) and (4).

The bordered sutured structure on the tangle exterior. The framing Φ of a Conway tangle T enables us to distinguish between the two components of $\partial B^3 \setminus \Phi$: The *front* is the component where the labelling of the points 1, 2, 3, 4 increases in counter-clockwise direction when viewed from outside B^3 ; we call the other component the *back* of T . On both front and back, we now choose a small disc whose boundary we may consider as a suture. We connect the two discs by four arcs $\beta_a, \beta_b, \beta_c,$ and β_d that each intersect the circle Φ only once, namely within the arcs $\alpha_a, \alpha_b, \alpha_c,$ and α_d , respectively. As in the case of the suture on the knot complement X_K in the previous subsection, we label the elementary paths on the front (resp. back) suture by p_i (resp. q_i) if they are adjacent to the tangle end labelled i . We now place basepoints on the elementary paths labelled p_4 and q_3 . Finally, we remove a sufficiently small open tubular neighbourhood of the tangle T that avoids the arcs $\beta_a, \beta_b, \beta_c,$ and β_d and the sutures. We denote the result by $X_T := B^3 \setminus \text{int}(\nu(T))$, the exterior of the tangle T . Since T is a tangle of horizontal connectivity, the basepoints lie in different components of the complement of the sutures and arcs on ∂X_T . Hence the arc diagram \mathcal{Z}_β consisting of the sutures with basepoints and the β -arcs $\beta_a, \beta_b, \beta_c,$ and β_d embedded on ∂X_T gives rise to a well-defined bordered sutured structure on X_T . This is illustrated in Figure 6b. Now the algebraic invariant corresponding to the multicurve γ_T is the associated type D structure $\widehat{\text{BSD}}(X_T)^\mathcal{B}$. For the construction of $\widehat{\text{BSD}}(X_T)^\mathcal{B}$, we refer the reader to [Zar11]; we only recall its formal properties, following [Zib20, Zib19b] and specializing to the case that the tangle T satisfies (3) and (4).

The peculiar algebra. $\widehat{\text{BSD}}(X_T)^\mathcal{B}$ is a graded chain complex over the bordered sutured algebra $\mathcal{A}(\mathcal{Z}_\beta, 1)$ with one moving strand, which can be identified with the quiver algebra

$$\mathcal{B} := \mathcal{A}_{43}^\partial = \mathbb{F}_2 \left[\begin{array}{ccc} & d & \\ q_1 \nearrow & & \nwarrow q_4 \\ a & p_1 & c \\ q_2 \searrow & & \swarrow p_3 \\ & b & \end{array} \right] / \left(p_i q_i = 0 = q_i p_i \right)_{i=1,2}.$$

We denote the idempotents in \mathcal{B} by $\iota_a, \iota_b, \iota_c,$ and ι_d , respectively. We also write $p_{12} := p_1 p_2, p_{23} := p_2 p_3, p_{123} := p_1 p_2 p_3, q_{21} := q_2 q_1, q_{32} := q_3 q_2,$ and $q_{321} := q_3 q_2 q_1$. This algebra carries two gradings, a $\frac{1}{2}\mathbb{Z}$ -grading δ determined by

$$\delta(p_1) = \delta(p_2) = \delta(p_3) = \frac{1}{2} = \delta(q_1) = \delta(q_2) = \delta(q_4)$$

and a \mathbb{Z}^2 -grading, called the Alexander grading, determined by

$$-A(p_1) = -A(q_1) = (1, 0) = A(q_4) \quad -A(p_2) = -A(q_2) = (0, 1) = A(p_3).$$

The chain complex $\widehat{\text{BSD}}(X_T)^\mathcal{B}$ is equipped with a δ -grading, which increases along the differential by 1, and an Alexander grading, which is preserved along the differential. We sometimes denote elements in this bigrading by $[r; a_1, a_2]$, where

$r \in \frac{1}{2}\mathbb{Z}$ is the δ -grading and $(a_1, a_2) \in \mathbb{Z}^2$ is the Alexander grading. We sometimes indicate the bigrading of a generator x using super- and subscripts: ${}^r x_{a_2}^{a_1}$. Given a bigraded chain complex C over \mathcal{B} , let $\delta^r t_1^{a_1} t_2^{a_2} C$ denote the chain complex obtained from C by increasing the Alexander and δ -gradings of all generators by (a_1, a_2) and r , respectively.

Classification result. To describe the classification of graded chain complexes over \mathcal{B} , we introduce a decoration of ∂X_T which is in some sense “dual” to the bordered sutured structure described above. We consider the tangle exterior with a meridional suture around each tangle end. The sutures decompose ∂X_T into a four-punctured sphere S_4^2 and two annuli. The four arcs $\alpha_a, \alpha_b, \alpha_c,$ and α_d of the framing Φ restrict to four arcs on ∂X_T , which we denote by the same combination of letters. We label the elementary path on the suture corresponding to the tangle end \mathbf{i} along the front (resp. back) by p_i (resp. q_i). Finally, we place basepoints on the elementary paths labelled p_4 and q_3 . This is illustrated on the right of Figure 2. (Note that with minor modifications, this can be turned into an actual bordered sutured structure: First, one adds basepoints to the sutures at the tangle ends 1 and 2; second, one also adds two arcs around those basepoints such that the corresponding gluing surface remains a four-punctured sphere; for details, see the proof of [Zib20, Theorem 3.7]. The simpler bordered sutured structure on X_T that we use in this paper was first introduced in [Zib19b, Section 5].)

As for curves on the one-punctured torus and complexes over the algebra \mathcal{A} , every non-contractible and primitive immersed curve (with or without local system) on the four-punctured sphere S_4^2 gives rise to a chain complex over \mathcal{B} . Chain complexes arising from curves with local systems are again *extendable* and we have the following result, which is apparent from [Zib19b, Theorem 5.3].

THEOREM 2.8. $\widehat{\text{BSD}}(X_T)^\mathcal{B}$ is extendable for every Conway tangle T satisfying (3) and (4).

The following result is [Zib20, Theorem 0.4].

THEOREM 2.9. Every extendable graded chain complex over \mathcal{B} is chain homotopic to a chain complex corresponding to a collection of curves on S_4^2 with (possibly trivial) local systems. This collection of curves is unique up to the equivalence from Definition 2.3.

Combining these two results, we now define:

Definition 2.10. For any Conway tangle T satisfying (3) and (4), let γ_T denote the collection of immersed curves with local systems on ∂X_T corresponding to $\widehat{\text{BSD}}(X_T)^\mathcal{B}$.

PROOF OF THEOREM 1.3. By the gluing formula [Zib20, Theorem 5.9], the Lagrangian Floer homology of γ_{T_K} with a rational curve of slope ∞ (a simple closed curve lifting to a straight line of slope ∞ in the planar cover) computes $\mathbb{F}_2^2 \otimes \widehat{\text{HF}}\mathbb{K}(U) \cong \mathbb{F}_2^2$. Combining this with the classification of components [Zib19b, Theorem 0.5] and detection of tangle connectivity [Zib20, Observation 6.1], we see that γ_{T_K} consists of exactly one rational component of even integer slope with the trivial one-dimensional local system and a (potentially vanishing) number of special components of slope ∞ with trivial local systems. The second part follows from [Zib19b, Theorem 0.10]. \square

2.3. Gradings. Recall from [Zar11] that in bordered (sutured) Heegaard Floer theory, the unreduced grading gr (aka unrefined grading gr' in the terminology of [LOT18]) of the algebra $\mathcal{A}(\mathcal{Z})$ associated with an arc diagram $\mathcal{Z} = (\mathbf{Z}, \mathbf{a}, M)$ takes values in the non-commutative group $\text{Gr}(\mathcal{Z})$, which is defined as a certain semi-direct product $\frac{1}{2}\mathbb{Z} \rtimes H_1(\mathbf{Z}, \mathbf{a})$. For convenience, we enlarge the grading set by working with rational coefficients, i.e. we replace $\text{Gr}(\mathcal{Z})$ by $\text{Gr}(\mathcal{Z}) \otimes \mathbb{Q} = \mathbb{Q} \rtimes H_1(\mathbf{Z}, \mathbf{a}; \mathbb{Q})$. There is also a reduced (refined) grading $\underline{\text{gr}}$ of $\mathcal{A}(\mathcal{Z})$, which takes values in $\underline{\text{Gr}}(\mathcal{Z})$, which we define as $\mathbb{Q} \rtimes H_1(\mathcal{F}(\mathcal{Z}); \mathbb{Q})$, where $\mathcal{F}(\mathcal{Z})$ is the surface obtained by thickening the arc diagram \mathcal{Z} . By default, we work with the gradings associated with type A sides.

Identification with the usual grading on the knot invariant. From [LOT18, Section 11.1], recall the reduced grading

$$\underline{\text{Gr}}(\mathcal{Z}_\alpha) := \mathbb{Q} \rtimes H_1(\mathcal{F}(\mathcal{Z}_\alpha); \mathbb{Q}) \cong \mathbb{Q} \times \mathbb{Q}^2$$

with the group law defined by

$$(j_1; p_1, q_1) \cdot (j_2; p_2, q_2) = \left(j_1 + j_2 - \det \begin{pmatrix} p_1 & q_1 \\ p_2 & q_2 \end{pmatrix}; p_1 + p_2, q_1 + q_2 \right)$$

for any $(j_i; p_i, q_i) \in \underline{\text{Gr}}(\mathcal{Z}_\alpha)$, $i = 1, 2$. (When comparing this formula with [LOT18, Section 11.1], note that the minus sign in front of the determinant comes from the fact that our algebra \mathcal{A} is the opposite algebra of the usual torus algebra; see Remark 2.1.) The grading on \mathcal{A} is defined by

$$\underline{\text{gr}}(\sigma_1) = (-\frac{1}{2}; \frac{1}{2}, -\frac{1}{2}) \quad \underline{\text{gr}}(\sigma_2) = (-\frac{1}{2}; \frac{1}{2}, \frac{1}{2}) \quad \underline{\text{gr}}(\sigma_3) = (-\frac{1}{2}; -\frac{1}{2}, \frac{1}{2})$$

The grading on $\widehat{\text{CFD}}(X_K)^{\mathcal{A}}$ takes values in the coset $\mathcal{P}_1 \backslash \underline{\text{Gr}}(\mathcal{Z}_\alpha)$, where \mathcal{P}_1 is the subgroup generated by $(-\frac{1}{2}; -1, 0)$. Moreover, it suffices to specify the grading of the generators in idempotent ι_\bullet , which are in bijection with the $(\mathbb{Q}^2$ -graded) generators of $\widehat{\text{HFK}}(K)$. (These two facts are explained in [LOT18, Theorem 11.26 and Remark 11.28], noting that by Theorem 2.5, the twisting parameter n can be chosen to be 0.) The first \mathbb{Q} -grading on $\widehat{\text{HFK}}(K)$ is called the δ -grading and the second \mathbb{Q} -grading is called the Alexander grading A . We will write $[m; n]$ for an element $(m, n) \in \mathbb{Q}^2$ of this bigrading. (Often, the Maslov grading M is considered instead of the δ -grading; one can be determined from the other using the identity $M + \delta = A$.) Then if \mathbf{x} is a (homogeneous) generator of $\widehat{\text{HFK}}(K)$ corresponding to a generator \mathbf{x}_0 of $\widehat{\text{CFD}}(X_K) \cdot \iota_\bullet$, then

$$\begin{aligned} \underline{\text{gr}}(\mathbf{x}_0) &= (M(\mathbf{x}) - \frac{3}{2}A(\mathbf{x}); 0, -A(\mathbf{x})) \\ &= (-\delta(\mathbf{x}) - \frac{1}{2}A(\mathbf{x}); 0, -A(\mathbf{x})) \in \mathcal{P}_1 \backslash \underline{\text{Gr}}(\mathcal{Z}_\alpha). \end{aligned}$$

Given a bigraded chain complex C over \mathcal{A} and $r, a \in \mathbb{Q}$, let $\delta^r t^a C$ denote the chain complex obtained from C by increasing the δ - and Alexander gradings of all generators by r and a , respectively.

Identification with the usual grading on the tangle invariant. Let T be a Conway tangle satisfying (3) and (4). The arc diagram $\mathcal{Z}_\beta = (\mathbf{Z}_\beta, \mathbf{a}_\beta, M_\beta)$ on the tangle exterior X_T is shown in Figure 4. The surface $\mathcal{F}(\mathcal{Z}_\beta)$ is a four-punctured sphere; in particular, it is planar. Hence, the intersection pairing on $H_1(\mathcal{F}(\mathcal{Z}_\beta))$ is trivial and $\underline{\text{Gr}}(\mathcal{Z}_\beta)$ is actually identical to $\mathbb{Q} \times H_1(\mathcal{F}(\mathcal{Z}_\beta); \mathbb{Q})$ as a group. To determine the reduced grading on the algebra $\mathcal{B} = \mathcal{A}(\mathcal{Z}_\beta)$, we choose the paths $\{p_1, p_2, p_3, q_2, q_1, q_4\}$

as a basis for $H_1(\mathbf{Z}_\beta, \mathbf{a}_\beta; \mathbb{Q})$ so that the unreduced gradings of the algebra generators are as follows:

$$\begin{aligned} \text{gr}(p_1) &= (-\tfrac{1}{2}; 1, 0, 0; 0, 0, 0), & \text{gr}(q_2) &= (-\tfrac{1}{2}; 0, 0, 0; 1, 0, 0), \\ \text{gr}(p_2) &= (-\tfrac{1}{2}; 0, 1, 0; 0, 0, 0), & \text{gr}(q_1) &= (-\tfrac{1}{2}; 0, 0, 0; 0, 1, 0), \\ \text{gr}(p_3) &= (-\tfrac{1}{2}; 0, 0, 1; 0, 0, 0), & \text{gr}(q_4) &= (-\tfrac{1}{2}; 0, 0, 0; 0, 0, 1). \end{aligned}$$

Recall from [Zib19b, Definition 1.7] the usual grading group \mathfrak{A} for \mathcal{B} , which we will replace by $\mathfrak{A} \otimes \mathbb{Q}$:

$$\mathfrak{A} := \mathbb{Q}^4 / \text{im}(\mathbb{Q} \rightarrow \mathbb{Q}^4, n \mapsto (n, n, n, n)).$$

We identify $H_1(\mathcal{F}(\mathcal{Z}_\beta); \mathbb{Q})$ with \mathfrak{A} via the homomorphism from \mathfrak{A} to $H_1(\mathcal{F}(\mathcal{Z}_\beta); \mathbb{Q})$ defined by

$$\begin{aligned} (1, 0, 0, 0) &\mapsto (\tfrac{1}{2}, 0, 0; 0, \tfrac{1}{2}, 0), & (0, 1, 0, 0) &\mapsto (0, \tfrac{1}{2}, 0; \tfrac{1}{2}, 0, 0), \\ (0, 0, 1, 0) &\mapsto (0, 0, \tfrac{1}{2}; -\tfrac{1}{2}, -\tfrac{1}{2}, -\tfrac{1}{2}), & (0, 0, 0, 1) &\mapsto (-\tfrac{1}{2}, -\tfrac{1}{2}, -\tfrac{1}{2}; 0, 0, \tfrac{1}{2}). \end{aligned}$$

We now choose a grading reduction r with ι_a as the base idempotent (so $r(\iota_a) = 0$) and

$$\begin{aligned} r(\iota_b) &= (0; 0, -\tfrac{1}{2}, 0; \tfrac{1}{2}, 0, 0), \\ r(\iota_c) &= (-\tfrac{1}{2}; 0, -\tfrac{1}{2}, -\tfrac{1}{2}; 0, -\tfrac{1}{2}, -\tfrac{1}{2}), \\ r(\iota_d) &= (0; \tfrac{1}{2}, 0, 0; 0, -\tfrac{1}{2}, 0). \end{aligned}$$

Given a basic algebra element $\xi = \iota_t \cdot \xi \cdot \iota_s \in \mathcal{B}$ for some $t, s \in \{a, b, c, d\}$, the reduced grading is computed using the formula

$$(2.1) \quad \underline{\text{gr}}(\xi) = (r(\iota_t))^{-1} \text{gr}(\xi) r(\iota_s).$$

An elementary calculation shows that the induced reduced grading is given by

$$\begin{aligned} \underline{\text{gr}}(p_1) &= \underline{\text{gr}}(q_1) = (-\tfrac{1}{2}; 1, 0, 0, 0), & \underline{\text{gr}}(p_3) &= (-\tfrac{1}{2}; 0, 0, 1, 0), \\ \underline{\text{gr}}(p_2) &= \underline{\text{gr}}(q_2) = (-\tfrac{1}{2}; 0, 1, 0, 0), & \underline{\text{gr}}(q_4) &= (-\tfrac{1}{2}; 0, 0, 0, 1). \end{aligned}$$

(To determine $\underline{\text{gr}}(p_3)$ and $\underline{\text{gr}}(q_4)$, it might be easier to compute $\underline{\text{gr}}(p_{23})$ and $\underline{\text{gr}}(q_{14})$ first.) Finally, since the tangle T satisfies (3) and (4), we simplify the grading further via the homomorphism $\varphi: \mathfrak{A} \rightarrow \mathbb{Q}^2$ sending

$$\begin{aligned} (1, 0, 0, 0) &\mapsto (-1, 0), & (0, 0, 0, 1) &\mapsto (1, 0), \\ (0, 1, 0, 0) &\mapsto (0, -1), & (0, 0, 1, 0) &\mapsto (0, 1). \end{aligned}$$

Then the gradings (δ, A) and $((-\text{id}_{\mathbb{Q}}) \times \varphi) \circ \underline{\text{gr}}$ on the algebra \mathcal{B} agree.

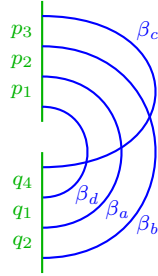


FIGURE 4. The arc diagram \mathcal{Z}_β for the bordered sutured structure on X_T

The grading on $\widehat{\text{BSD}}(X_T)$ takes values in $\mathcal{P}_2 \setminus \underline{\text{Gr}}(\mathcal{Z}_\beta)$, where \mathcal{P}_2 is the subgroup $\underline{\text{gr}}(\pi_2(\mathbf{x}, \mathbf{x}; \mathbb{Q}))$ defined as follows: First we fix a Heegaard diagram for X_T and we pick some base generator \mathbf{x} of $\widehat{\text{BSD}}(X_T)_{\iota_a}$. (This is always possible.) We now consider $\pi_2(\mathbf{x}, \mathbf{x}; \mathbb{Q})$, the group of periodic domains on a Heegaard diagram for X_T (with coefficients in \mathbb{Q}). Each domain B has a certain unreduced grading $\text{gr}(B)$. Let $R(\text{gr}(B))$ be the element of $\text{Gr}(\mathcal{Z}_\beta)$ obtained from $\text{gr}(B)$ by multiplying all components except the first by -1 . Then we define $\underline{\text{gr}}(B)$ as the element of $\underline{\text{Gr}}(\mathcal{Z}_\beta)$ corresponding to $R(\text{gr}(B))$ using the above grading reduction r . \mathcal{P}_2 is now the subgroup generated by the elements $\underline{\text{gr}}(B)$ for all periodic domains $B \in \pi_2(\mathbf{x}, \mathbf{x}; \mathbb{Q})$. To understand this subgroup better, we choose a Heegaard diagram with a single α -circle parallel to the front suture. (This is always possible.) The periodic domains of such a Heegaard diagram are generated by a single domain ψ . An elementary computation (similar to the proof of [Zib19a, Lemma 5.12]) shows that the reduced grading of ψ is equal to $\pm(0; 1, 0, 0, 1)$. Hence, we can use the above identification of the gradings on the algebra \mathcal{B} to also identify the gradings on $\widehat{\text{BSD}}(X_T)$. (Alternatively, in the case that T is a double tangle T_K for some knot K , this identification will also emerge from the proof of Theorem 3.1).

3. Computations in bordered sutured Heegaard Floer theory

The goal of this section is to prove the following result.

THEOREM 3.1. *Let X_K be the complement of an open tubular neighbourhood of a knot K in S^3 . We equip ∂X_K with the standard bordered parametrization by meridian and longitude. Then*

$$\widehat{\text{BSD}}(X_{T_K})^{\mathcal{B}} \cong \widehat{\text{CFD}}(X_K)^{\mathcal{A}} \boxtimes {}_{\mathcal{A}}\mathcal{Y}^{\mathcal{B}},$$

where ${}_{\mathcal{A}}\mathcal{Y}^{\mathcal{B}}$ is the type AD bimodule shown in Figure 5. The reduced grading of ${}_{\mathcal{A}}\mathcal{Y}^{\mathcal{B}}$ takes values in $(\underline{\text{Gr}}(\mathcal{Z}_\alpha) \times \mathfrak{A})/\mathcal{P}_3$ where \mathcal{P}_3 is the subgroup generated by

$$(0; 0, 0; 0, 1, 1, 0) \quad \text{and} \quad (-\tfrac{1}{2}; 0, 1; 0, 0, 2, 2).$$

Moreover, if $\underline{\text{gr}}(a) = \mathcal{P}_3$ then $\underline{\text{gr}}(c) = (-\tfrac{1}{2}; -1, 0; 0, 0, 0, 0) \cdot \mathcal{P}_3$.

PROOF. Consider the bordered sutured manifold Y shown in Figure 6c. Gluing Y to the knot complement X_K shown in Figure 6a produces the tangle complement X_{T_K} equipped with the bordered sutured structure described in Section 2 and shown in Figure 6b. By the pairing theorem [Zar11, Theorem 12.3.2],

$$\widehat{\text{BSD}}(X_{T_K})^{\mathcal{B}} = \widehat{\text{CFD}}(X_K)^{\mathcal{A}} \boxtimes {}_{\mathcal{A}}\widehat{\text{BSAD}}(Y)^{\mathcal{B}}.$$

(Here, ${}_{\mathcal{A}}\widehat{\text{BSAD}}(Y)^{\mathcal{B}}$ denotes the direct summand of the type AD structure $\widehat{\text{BSAD}}(Y)$ whose generators occupy exactly one of α_μ and α_λ .) So it suffices to show that ${}_{\mathcal{A}}\mathcal{Y}^{\mathcal{B}}$ and ${}_{\mathcal{A}}\widehat{\text{BSAD}}(Y)^{\mathcal{B}}$ are graded chain homotopic. In fact, we will show that

$${}_{\mathcal{A}}\mathcal{Y}^{\mathcal{B}} = {}_{\mathcal{A}}\widehat{\text{BSAD}}(\mathcal{H}_Y)^{\mathcal{B}}$$

for the Heegaard diagram \mathcal{H}_Y of Y shown in Figure 6d.

The type AD structure ${}_{\mathcal{A}}\widehat{\text{BSAD}}(\mathcal{H}_Y)^{\mathcal{B}}$ consists of eight generators in total. We name the generators by the concatenation of the intersection points they are composed of. They are shown as the vertices of the graph in Figure 7. The idempotents of \mathcal{A} acting on the generators on the left can be read off the subscript

of the first letter: The four generators in middle two columns lie in the meridional idempotent ι_\bullet , the other four generators belong to the longitudinal idempotent ι_\circ . The basic idempotents of \mathcal{B} acting on the generators on the right can also be deduced from the name: A generator belongs to idempotent ι_x for $x \in \{a, b, c, d\}$ if the letter x does not appear in the name. (This is also indicated by the colours.)

Next, we consider the regions in the Heegaard diagram. As for the generators, we use suggestive notation and label them by algebra elements of \mathcal{B} and \mathcal{A} , i.e. p_i , q_j , and σ_ℓ , or combinations thereof. In the following, let us write domains D as formal differences $D_+ - D_-$ of unordered multisets of regions D_+ and D_- with $D_+ \cap D_- = \emptyset$ such that

$$D = \sum_{r \in D_+} r - \sum_{r \in D_-} r.$$

Let us calculate some connecting domains between the generators. The solid arrows in Figure 7 indicate some n -gons with boundary punctures, which contribute to the type AD structure. Furthermore, elementary combinatorial arguments show that the group of periodic domains of \mathcal{H}_Y is freely generated by the domains

$$B_1 := \{q_1, q_4\} - \{p_2, p_3\}, \quad \text{and} \quad B_2 := \{\sigma_2, \sigma_3/p_1, p_2, q_1, q_2\}.$$

Figure 7 shows all connecting domains satisfying the following conditions: the multiplicity of each region is non-negative; the multiplicity of each region labelled by p_i and q_j is at most 1; the multiplicity 1 regions do not include *both* those labelled by p_i and q_j . (This follows from routine calculations, most of which can be outsourced to a computer using the python script [Zib22].) These are the only domains that can possibly contribute to the differential in the type AD structure $\widehat{\mathcal{A}}\text{BSAD}(\mathcal{H}_Y)^\mathcal{B}$, but we do not know (yet) whether they do. However, it turns out, this is all we need to compute from the Heegaard diagram.

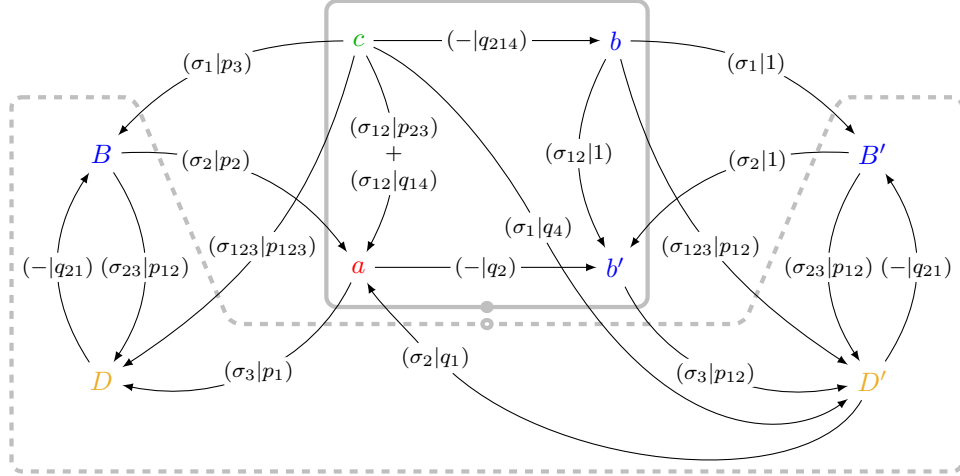


FIGURE 5. The type AD bimodule $\mathcal{A}\mathcal{Y}^\mathcal{B}$. The right idempotents of the generators are determined by the letter of the generator names; for example, the right idempotent of the generator named B' is ι_b . Generators named by a lower-case letter sit in the left idempotent ι_\bullet , those named by an upper-case letter belong to the left idempotent ι_\circ .

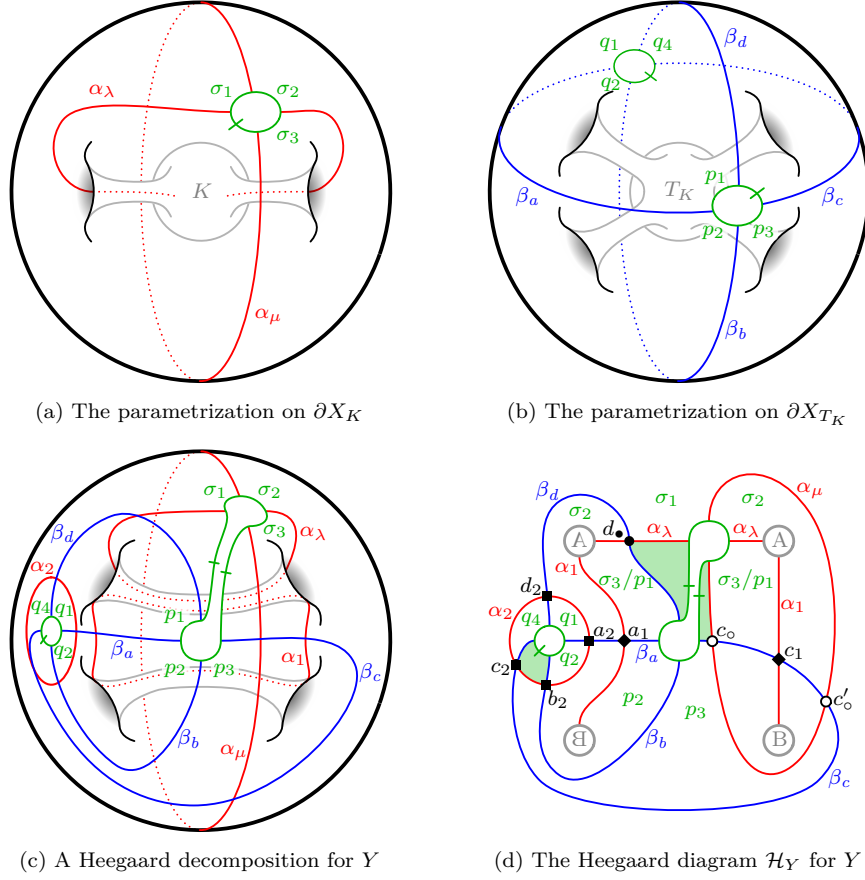


FIGURE 6. The tangle complement X_{T_K} (b) is obtained from the knot complement X_K (a) by gluing the bordered sutured manifold Y (c) to it. Figure (d) shows a Heegaard diagram from which we compute the type AD bimodule ${}_{\mathcal{A}}\mathcal{Y}^{\mathcal{B}}$.

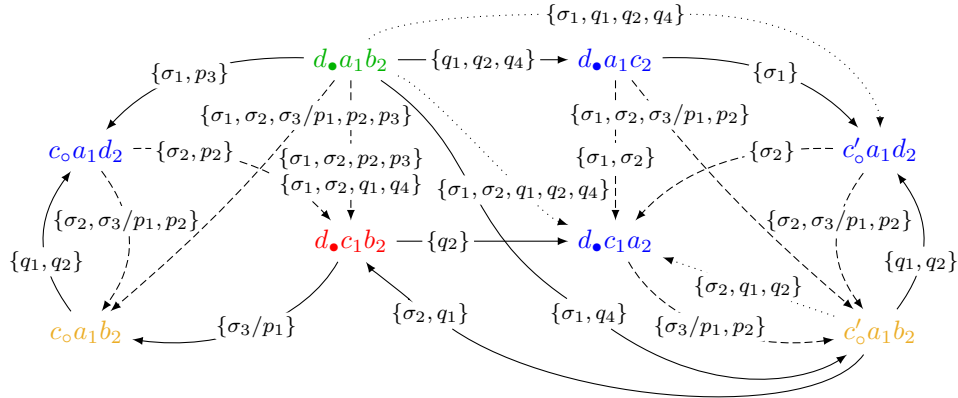


FIGURE 7. Domains connecting generators

domain B	$e(B)$	$n_x(B)$	$n_y(B)$	$\#\vec{\rho}_1$	$\#\vec{\rho}_2$	$\iota(\rho_1)$	$\iota(\rho_2)$	$\text{ind}(B, \vec{\rho}_1, \vec{\rho}_2)$
$\{\sigma_1, q_1, q_2, q_4\}$	$-\frac{1}{2}$	$\frac{1}{2}$	1	1	1	$-\frac{1}{2}$	$-\frac{1}{2}$	2
$\{\sigma_2, q_1, q_2\}$	-1	$\frac{3}{4}$	$\frac{5}{4}$	1	1	$-\frac{1}{2}$	$-\frac{1}{2}$	2
$\{\sigma_1, \sigma_2, q_1, q_2, q_4\}$	$-\frac{3}{2}$	1	$\frac{3}{2}$	1	≥ 1	$-\frac{1}{2}$	$-\frac{1}{2}$	≥ 2

FIGURE 8. Computation of the embedded indices of the domains on the dotted arrows in Figure 7 following [Zar11, Definition 8.4.2]. Here, $B \in \pi_2(\mathbf{x}, \mathbf{y})$ denotes a domain connecting two generators \mathbf{x} and \mathbf{y} . The symbols $\vec{\rho}_1$ and $\vec{\rho}_2$ denote sets of Reeb chords on the type D side and type A side, respectively.

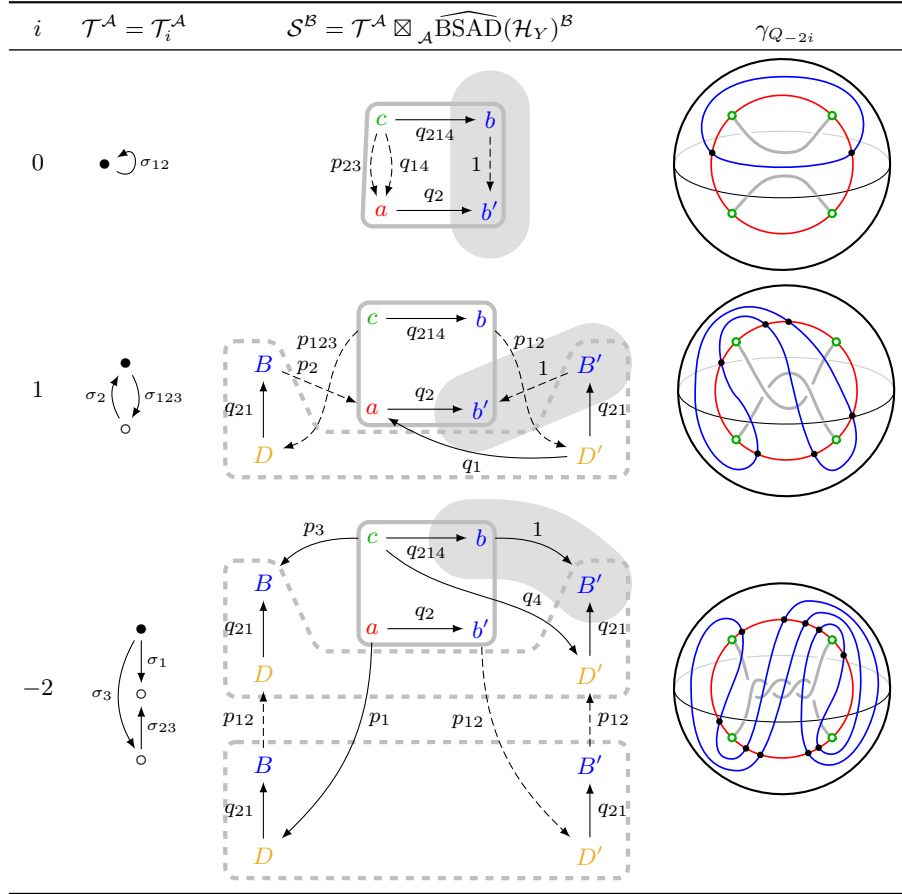


FIGURE 9. Test pairings to determine which pseudoholomorphic curves contribute to the differential in $\widehat{\mathcal{A}}\text{BSAD}(\mathcal{H}_Y)^B$. Specifically, the dashed arrows originate from the problematic differentials in $\widehat{\mathcal{A}}\text{BSAD}(\mathcal{H}_Y)^B$. Likewise, the solid arrows correspond to the unproblematic differentials. The highlighted arrows labelled 1 can be cancelled using [Zib20, Lemma 1.22]. A comparison of the last two columns demonstrates that indeed, all dashed arrows have to be part of the differential of \mathcal{S}^B .

The domains on the three dotted arrows do not contribute to the differential $\widehat{{}_A\text{BSAD}}(\mathcal{H}_Y)^{\mathcal{B}}$, because the expected dimension of the corresponding moduli spaces is not 1; see Figure 8. Comparing Figures 5 and 7, it remains to see that all dashed arrows contribute to the differential. We check this indirectly by pairing $\widehat{{}_A\text{BSAD}}(\mathcal{H}_Y)^{\mathcal{B}}$ with certain test type D structures \mathcal{T}^A for which we already know the result

$$\mathcal{S}^{\mathcal{B}} := \mathcal{T}^A \boxtimes \widehat{{}_A\text{BSAD}}(\mathcal{H}_Y)^{\mathcal{B}}$$

up to homotopy. To construct such \mathcal{T}^A , let $X_K(i)$ be the knot complement equipped with the bordered structure given by the meridian μ and the longitude $\lambda + i\mu$, where λ is the homological longitude. Then, setting $K = U$ and $\mathcal{T} = \mathcal{T}_i = \widehat{\text{CFD}}(X_U(i))$, we know that $\mathcal{S}^{\mathcal{B}}$ is chain homotopic to $\widehat{\text{BSD}}(X_{Q_{-2i}})^{\mathcal{B}}$, where Q_{-2i} is the rational tangle of slope $-2i$. Figure 9 compares the expected and the computed result for $\mathcal{S}^{\mathcal{B}}$ for some values of i . We conclude that all dashed arrows need to contribute, which concludes the identification of $\widehat{{}_A\text{BSAD}}(\mathcal{H}_Y)^{\mathcal{B}}$ with ${}_A\mathcal{Y}^{\mathcal{B}}$, up to gradings.

So it remains to consider gradings. The unreduced grading of $\widehat{{}_A\text{BSAD}}(\mathcal{H}_Y)^{\mathcal{B}}$ takes values in $\mathbb{Q} \times H_1(\mathbf{Z}_\alpha, \mathbf{a}_\alpha; \mathbb{Q}) \times H_1(\mathbf{Z}_\beta, \mathbf{a}_\beta; \mathbb{Q})$. The unreduced grading gr of the periodic domains $B_1, B_2 \in \pi_2(\mathbf{d}_\bullet \mathbf{c}_1 \mathbf{b}_2, \mathbf{d}_\bullet \mathbf{c}_1 \mathbf{b}_2)$ is equal to

$$\text{gr}(B_1) = (0; 0, 0, 0; 0, -1, -1; 0, 1, 1) \quad \text{and} \quad \text{gr}(B_2) = (-\tfrac{1}{2}; 0, 1, 1; 1, 1, 0; 1, 1, 0)$$

and the unreduced grading of the domain $B_3 = \{\sigma_1, \sigma_2, p_2, p_3\} \in \pi_2(\mathbf{d}_\bullet \mathbf{a}_1 \mathbf{b}_2, \mathbf{d}_\bullet \mathbf{c}_1 \mathbf{b}_2)$ is equal to

$$\text{gr}(B_3) = (0; 1, 1, 0; 0, 1, 1; 0, 0, 0).$$

Using the same grading reductions as in Section 2 (after multiplying the components of $H_1(\mathbf{Z}_\beta, \mathbf{a}_\beta; \mathbb{Q})$ by -1), the reduced gradings of these three domains is

$$\underline{\text{gr}}(B_1) = (0; 0, 0; 0, 2, 2, 0) \quad \text{and} \quad \underline{\text{gr}}(B_2) = (-\tfrac{1}{2}; 0, 1; 0, 0, 2, 2)$$

and

$$\begin{aligned} \underline{\text{gr}}(B_3) &= (r(\iota_c))^{-1} R(\text{gr}(B_3)) \\ &= (\tfrac{1}{2}; 1, 1, 0; 0, -\tfrac{1}{2}, -\tfrac{1}{2}; 0, \tfrac{1}{2}, \tfrac{1}{2}) = (\tfrac{1}{2}; 1, 0; 0, -1, -1, 0); \end{aligned}$$

compare [LOT18, Formulas 3.44 and 10.36] and (2.1). Let $\mathcal{P}_3 = \langle \underline{\text{gr}}(B_1), \underline{\text{gr}}(B_2) \rangle$ and choose \mathbf{a} as the base generator, i.e. $\underline{\text{gr}}(\mathbf{a}) = \mathcal{P}_3$. Then, since $-B_3 \in \pi_2(\mathbf{c}, \mathbf{a})$,

$$\begin{aligned} \underline{\text{gr}}(\mathbf{c}) &= \underline{\text{gr}}(-B_3) \cdot \mathcal{P}_3 \\ &= (-\tfrac{1}{2}; -1, 0; 0, 1, 1, 0) \cdot \mathcal{P}_3 = (-\tfrac{1}{2}; -1, 0; 0, 0, 0, 0) \cdot \mathcal{P}_3. \quad \square \end{aligned}$$

4. Proof of the Main Theorem

We now prove the following graded version of the Main Theorem.

THEOREM 4.1. *The components of γ_{T_K} are in one-to-one correspondence with the curve segments in $S_\times(\gamma_K)$ (Definition 2.7). More specifically, for any $r, a \in \frac{1}{2}\mathbb{Z}$ and $\ell \in \mathbb{Z}^{>0}$, we have the following correspondence:*

$$\text{in } \gamma_K \left\{ \begin{array}{l} \mathbf{d}_{2\tau(K)} \quad \longleftrightarrow \quad \mathbf{r}_{4\tau(K)} \\ \delta^r t^a \mathbf{u}_\ell \quad \longleftrightarrow \quad \delta^{r+a} t_1^{2a} t_2^{2a} \mathbf{s}_{2\ell} \\ \delta^r t^{-a} \mathbf{v}_\ell \quad \longleftrightarrow \quad \delta^{r+a} t_1^{-2a} t_2^{-2a} \bar{\mathbf{s}}_{2\ell} \end{array} \right\} \text{ in } \gamma_{T_K}$$

where the gradings on the curves/curve segments is as in Figures 10 and 11.

Example 4.2. For the right-handed trefoil knot $K = T_{2,3} = 3_1$,

$$S_{\infty}(\gamma_K) = \{\mathbf{d}_2, \delta^{\frac{3}{2}} t^{+\frac{1}{2}} \mathbf{u}_1, \delta^{\frac{3}{2}} t^{-\frac{1}{2}} \mathbf{v}_1\};$$

see for example [Han19]. Hence

$$\gamma_{T_K} = \mathbf{r}_4 \cup \delta^2 t_1^{+1} t_2^{+1} \mathbf{s}_2 \cup \delta^2 t_1^{-1} t_2^{-1} \bar{\mathbf{s}}_2.$$

As one might expect [KWZ21, Example 7.15], T_K is an example of a Heegaard Floer exceptional tangle, since $\delta(\mathbf{s}, \mathbf{r}_4) = 2$ for both special components \mathbf{s} of γ_{T_K} .

Example 4.3. For the figure-eight knot $K = 4_1$,

$$\begin{aligned} S_{\infty}(\gamma_K) &= \{\mathbf{d}_0, \delta^{\frac{1}{2}} t^{+\frac{1}{2}} \mathbf{u}_1, \delta^{\frac{1}{2}} t^{-\frac{1}{2}} \mathbf{u}_1, \delta^{\frac{1}{2}} t^{-\frac{1}{2}} \mathbf{v}_1, \delta^{\frac{1}{2}} t^{+\frac{1}{2}} \mathbf{v}_1\}, \\ \gamma_{T_K} &= \mathbf{r}_0 \cup \delta^1 t_1^{+1} t_2^{+1} \mathbf{s}_2 \cup \delta^0 t_1^{-1} t_2^{-1} \mathbf{s}_2 \\ &\quad \cup \delta^1 t_1^{-1} t_2^{-1} \bar{\mathbf{s}}_2 \cup \delta^0 t_1^{+1} t_2^{+1} \bar{\mathbf{s}}_2. \end{aligned}$$

Example 4.4. For the $(3, 4)$ -torus knot $K = T_{3,4} = 8_{19}$,

$$\begin{aligned} S_{\infty}(\gamma_K) &= \{\mathbf{d}_6, \delta^{\frac{7}{2}} t^{+\frac{5}{2}} \mathbf{u}_1, \delta^3 t^{-1} \mathbf{u}_2, \delta^{\frac{7}{2}} t^{-\frac{5}{2}} \mathbf{v}_1, \delta^3 t^{+1} \mathbf{v}_2\}, \\ \gamma_{T_K} &= \mathbf{r}_{12} \cup \delta^6 t_1^{+5} t_2^{+5} \mathbf{s}_2 \cup \delta^2 t_1^{-2} t_2^{-2} \mathbf{s}_4 \\ &\quad \cup \delta^6 t_1^{-5} t_2^{-5} \bar{\mathbf{s}}_2 \cup \delta^2 t_1^{+2} t_2^{+2} \bar{\mathbf{s}}_4. \end{aligned}$$

Remark 4.5. The curve segments \mathbf{d}_k in Figure 10 are graded such that for any knot K , $\mathbf{d}_{2\tau(K)}$ is equal to an element of $S_{\infty}(\gamma_K)$ without any additional grading shift. This is ensured by the symmetry with respect to the Alexander grading and the convention that the Maslov grading of the right generators \bullet in Figures 10c to 10e vanishes. (These are the generators that are mapped to the generators of $\widehat{\text{HF}}(S^3)$ under the spectral sequence corresponding to setting $U = 0$ and $V = 1$.)

Remark 4.6. The graded version of conjugation symmetry for the multicurve γ_K (Theorem 1.2) corresponds precisely to the graded version of conjugation symmetry for the multicurve γ_{T_K} (Theorem 1.3). Indeed, the former says that for any $\ell \in \mathbb{Z}^{>0}$ and $r, a \in \frac{1}{2}\mathbb{Z}$,

$$\begin{aligned} \#\{\text{curve segments } \delta^r t^a \mathbf{u}_\ell \text{ in } S_{\infty}(\gamma_K)\} &= \#\{\text{curve segments } \delta^r t^{-a} \mathbf{v}_\ell \text{ in } S_{\infty}(\gamma_K)\} \\ \text{and the latter that for any } \ell \in \mathbb{Z}^{>0} \text{ and } r, a_1, a_2 \in \frac{1}{2}\mathbb{Z}, \end{aligned}$$

$$\#\{\text{components } \delta^r t_1^{a_1} t_2^{a_2} \mathbf{s}_{2\ell} \text{ of } \gamma_{T_K}\} = \#\{\text{components } \delta^r t_1^{-a_1} t_2^{-a_2} \bar{\mathbf{s}}_{2\ell} \text{ of } \gamma_{T_K}\}.$$

PROOF OF THEOREM 4.1. Let us assume first that all local systems on γ_K are one-dimensional and thus trivial. With a view towards applying Theorem 3.1, we first compute the effect of applying $-\boxtimes_{\mathcal{A}} \mathcal{Y}^{\mathcal{B}}$ to the chain complexes over \mathcal{A} corresponding to curve segments, ignoring gradings for a moment. We carry out these computations in Figure 12. Clearly, $\mathbf{u}_\ell \boxtimes_{\mathcal{A}} \mathcal{Y}^{\mathcal{B}}$ contains a direct summand that is chain homotopic to (the chain complex over \mathcal{B} corresponding to) $\mathbf{s}_{2\ell}$, and the same is true for $\mathbf{v}_\ell \boxtimes_{\mathcal{A}} \mathcal{Y}^{\mathcal{B}}$ and $\bar{\mathbf{s}}_{2\ell}$, as well as for $\mathbf{d}_k \boxtimes_{\mathcal{A}} \mathcal{Y}^{\mathcal{B}}$ and \mathbf{r}_{2k} for all $\ell \in \mathbb{Z}^{>0}$ and $k \in \mathbb{Z}$. However, in each case, four additional generators remain, two on each end, so to speak. This is where we make use of Hanselman and Watson's puzzle piece notation [HW15, Figure 1]. This notation is chosen such that two puzzle pieces fit together if and only if the corresponding curve segments can be joined at the respective ends to a valid curve on the torus. The following observation is crucial: At each male end of a puzzle piece, the remaining two generators are the

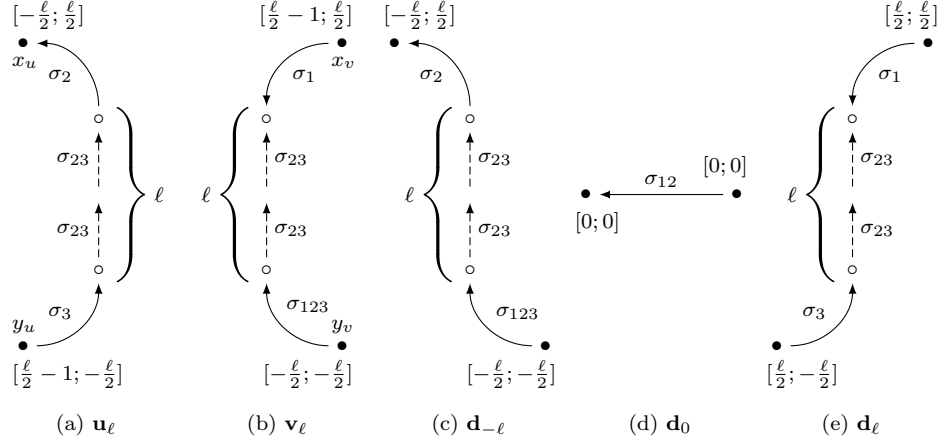


FIGURE 10. The graded chain complexes corresponding to the curve segments that can occur in $S_\infty(\gamma_K)$. Note $\ell \in \mathbb{Z}^{>0}$.

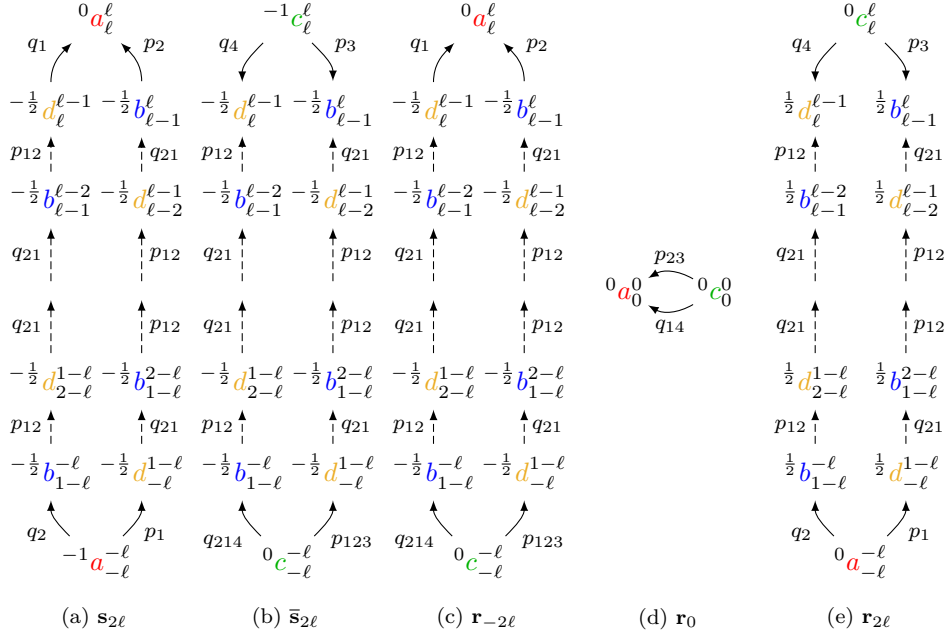


FIGURE 11. The graded chain complexes corresponding to curves that can appear as components of γ_{TK} . Note $\ell \in \mathbb{Z}^{>0}$.

same, namely c and b . Similarly, at the female ends, the generators a and b' remain. This justifies a posteriori that the computation of $\widehat{\text{CFD}}(X_K)^{\mathcal{A}} \boxtimes_{\mathcal{A}} \mathcal{Y}^{\mathcal{B}}$ can indeed be done locally on each curve segment. In other words, $\widehat{\text{CFD}}(X_K)^{\mathcal{A}} \boxtimes_{\mathcal{A}} \mathcal{Y}^{\mathcal{B}}$ is indeed a direct sum of chain complexes over \mathcal{B} , namely one for each curve segment, as stated in the correspondence. We now apply Theorem 3.1 to conclude.

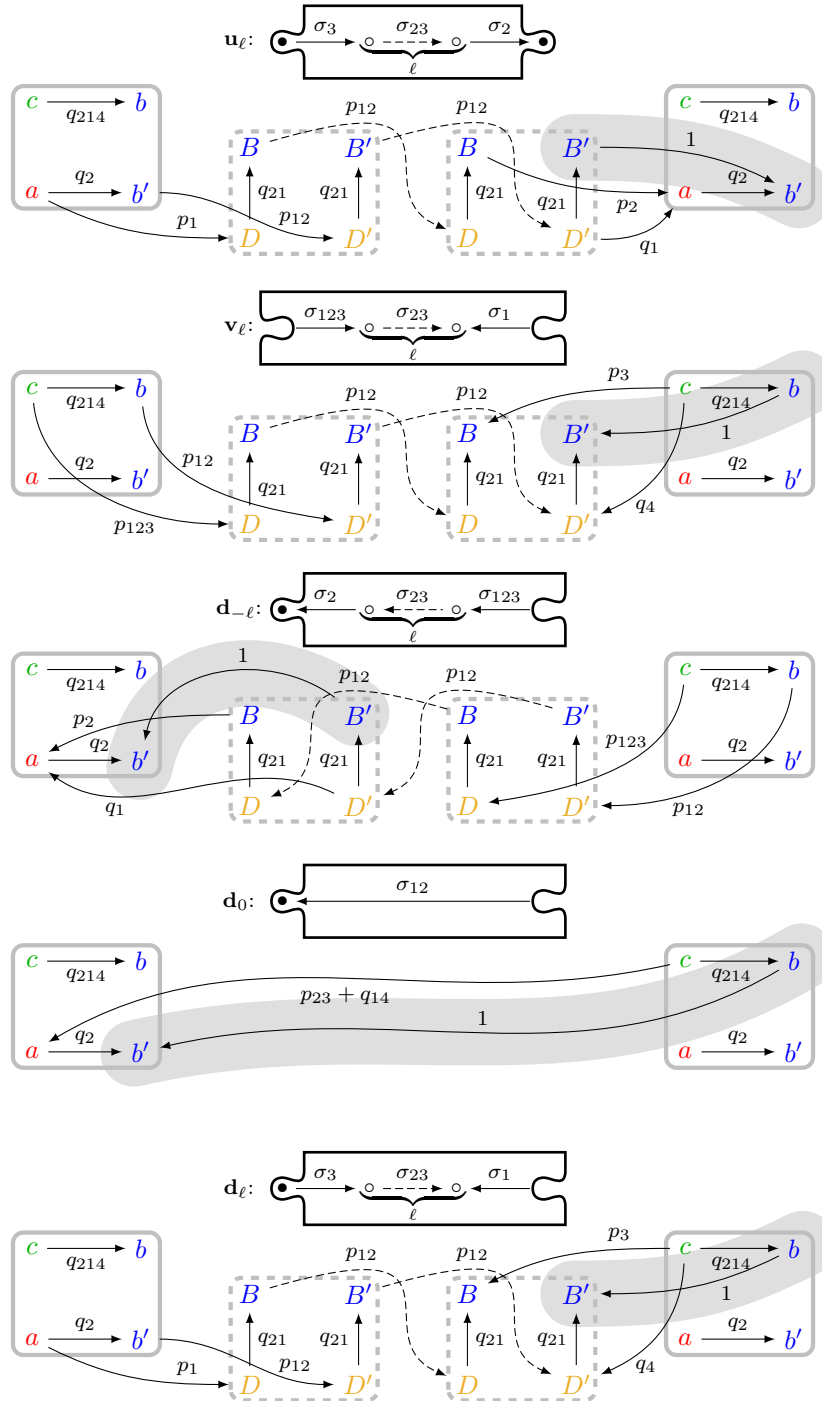


FIGURE 12. The main computation for the proof of Theorem 4.1, not including gradings. Each puzzle piece represents a curve segment in $S_-(\gamma_K)$, which, when tensored with the type AD structure ${}_A\mathcal{Y}^B$, becomes the chain complex over \mathcal{B} shown below the puzzle piece. Note $\ell \in \mathbb{Z}^{>0}$.

It remains to verify the gradings and to consider curves with non-trivial local systems. We start with the latter. Let us suppose that γ_K contains some component with higher-dimensional local system X . For convenience, we may put this local system on an arrow adjacent to a generator in idempotent \bullet ; see the discussion before Definition 2.3. By inspecting the complexes in Figure 12, we see that the local system on the curve corresponding to the curve segment containing this arrow is equal to $XX^{-1} = \text{id}$. So any local system has the same effect on the result as a trivial local system of the same dimension.

To check the gradings, it clearly suffices to compute the grading of the generators in idempotents a and c . Note that any element the double coset $\mathcal{P}_1 \backslash (\widehat{\text{Gr}}(\mathcal{Z}_\alpha) \times \mathfrak{A}) / \mathcal{P}_3$ can be uniquely written as $\mathcal{P}_1 \cdot (x; 0, 0; 0, 0, y, z) \cdot \mathcal{P}_3$ for some $x, y, z \in \mathbb{Q}$. Identifying this element with $[-x; y, z]$, this recovers the usual bigrading on the tangle invariant. So, given a generator of $\widehat{\text{CFD}}(X_K)^A \cdot \iota_\bullet$ in grading $[m; n]$, the corresponding generator of $\widehat{\text{CFD}}(X_K)^A \boxtimes_{\mathcal{A}} \mathcal{Y}^B$ in idempotent a has grading

$$\begin{aligned} & \mathcal{P}_1 \cdot (-m - \frac{n}{2}; 0, -n; 0, 0, 0, 0) \cdot \mathcal{P}_3 \\ &= \mathcal{P}_1 \cdot (-m - n; 0, 0; 0, 0, 2n, 2n) (\frac{1}{2}; 0, -1; 0, 0, -2, -2)^n \cdot \mathcal{P}_3 \\ &= \mathcal{P}_1 \cdot (-m - n; 0, 0; 0, 0, 2n, 2n) \cdot \mathcal{P}_3 \\ &= [m + n; 2n, 2n] \end{aligned}$$

and the corresponding generator in idempotent c has grading

$$\begin{aligned} & \mathcal{P}_1 \cdot (-m - \frac{n}{2}; 0, -n; 0, 0, 0, 0) (-\frac{1}{2}; -1, 0; 0, 0, 0, 0) \cdot \mathcal{P}_3 \\ &= \mathcal{P}_1 \cdot (-m - \frac{n}{2} - \frac{1}{2} + n; -1, -n; 0, 0, 0, 0) \cdot \mathcal{P}_3 \\ &= \mathcal{P}_1 \cdot (-\frac{1}{2}; -1, 0; 0, 0, 0, 0) (-m + n + \frac{n}{2}; 0, -n; 0, 0, 0, 0) \cdot \mathcal{P}_3 \\ &= \mathcal{P}_1 \cdot (-m + n; 0, 0; 0, 0, 2n, 2n) (\frac{1}{2}; 0, -1; 0, 0, -2, -2)^n \cdot \mathcal{P}_3 \\ &= \mathcal{P}_1 \cdot (-m + n; 0, 0; 0, 0, 2n, 2n) \cdot \mathcal{P}_3 \\ &= [m - n; 2n, 2n]. \end{aligned}$$

So it suffices to check the identities above for $r = 0 = a$. This is elementary to check, we simply compare the gradings in Figures 10 and 11. \square

5. Satellites, thinness, and A-links

We now prove the results from Subsection 1.5 of the introduction.

PROOF OF THEOREM 1.8. Zoltan Szabó's program [OS17] computes the following knot Floer homology of the knot K shown in Figure 3:

$$\widehat{\text{HFK}}(K) \cong \delta^0 t^1 \mathbb{F}^4 \oplus \delta^0 t^0 \mathbb{F}^9 \oplus \delta^0 t^{-1} \mathbb{F}^4.$$

A conceptually more interesting proof, which also explains how this example was found, uses the multicurve invariant of the double tangle of the trefoil knot computed in Example 4.2. Note that the Conway tangle T_\star highlighted on the left of Figure 3 agrees with said double tangle up to two full twists. Using the naturality of the multicurve invariant under twisting [Zib19b, Theorem 3.1], we see that γ_{T_\star} consists of a single rational component \mathbf{r}_0 of slope 0 and a pair of conjugate special components of slope ∞ , denoted here by \mathbf{S}_∞ . The complementary tangle T'_\star on the right of Figure 3 is obtained from T_\star by rotation in the plane about 90 degrees and reversing all crossings. Thus, the corresponding multicurve invariant consists

generator x	component of $S_\infty(\gamma_K)$	component of γ_{T_K}
x_u	$\delta^{r+\frac{\ell}{2}} t^{a-\frac{\ell}{2}} \mathbf{u}_\ell$	$\delta^{r+a} t_1^{2a-\ell} t_2^{2a-\ell} \mathbf{s}_{2\ell}$
y_u	$\delta^{r+1-\frac{\ell}{2}} t^{a+\frac{\ell}{2}} \mathbf{u}_\ell$	$\delta^{r+1+a} t_1^{2a+\ell} t_2^{2a+\ell} \mathbf{s}_{2\ell}$
x_v	$\delta^{r+1-\frac{\ell}{2}} t^{a-\frac{\ell}{2}} \mathbf{v}_\ell$	$\delta^{r+1-a} t_1^{2a-\ell} t_2^{2a-\ell} \bar{\mathbf{s}}_{2\ell}$
y_v	$\delta^{r+\frac{\ell}{2}} t^{a+\frac{\ell}{2}} \mathbf{v}_\ell$	$\delta^{r-a} t_1^{2a+\ell} t_2^{2a+\ell} \bar{\mathbf{s}}_{2\ell}$

FIGURE 13. Computations for the proof of Proposition 5.1.

of a single rational component \mathbf{r}_∞ of slope ∞ and a pair \mathbf{S}_0 of conjugate special components of slope 0. The Lagrangian Floer homology between a rational and a special component of the same slope is zero [KWZ21, Lemma 4.20]. Hence, by the gluing theorem [Zib20, Theorem 5.9],

$$\widehat{\text{HF}}\text{K}(T'_* \cup T_*) \otimes \mathbb{F}^2 \cong \text{HF}(-\gamma_{T'_*}, \gamma_{T_*}) \cong \text{HF}(-\mathbf{r}_\infty, \mathbf{r}_0) \oplus \text{HF}(-\mathbf{S}_0, \mathbf{S}_\infty).$$

These two summands are thin and supported in the same δ -grading. This can be seen either by direct computation or as an application of [KWZ21, Lemma 4.17]. \square

Proposition 5.1. *For any knot $K \subset S^3$ except the unknot and the trefoil knots, the multicurve γ_{T_K} contains two special components in distinct δ -gradings.*

PROOF. We first introduce some notation and make some preliminary computations. Given a curve segment \mathbf{u}_ℓ or \mathbf{v}_ℓ in $S_\infty(\gamma_K)$, consider the two generators of $\widehat{\text{HF}}\text{K}(K)$ at the ends of this curve segment. If the segment is of type \mathbf{u}_ℓ , we denote these two generators by x_u and y_u as shown in Figure 10a; if it is of type \mathbf{v}_ℓ , we denote them by x_v and y_v as shown in Figure 10b. The second column of the table in Figure 13 shows the graded curve segments whose generators $x \in \{x_u, y_u, x_v, y_v\}$, determined in the first column, sit in bigrading $[r; a]$. The third column shows the corresponding components of γ_{T_K} computed using Theorem 4.1. Note that the δ -grading of the components of γ_{T_K} are independent of the components' length ℓ .

We now study how two such curve segments can be joined up along a generator x of $\widehat{\text{HF}}\text{K}(K)$ to form part of the curve γ_K . We distinguish two cases:

- (1) Suppose $x = x_u = x_v$ or $x = y_u = y_v$. We compare the first and third, respectively second and fourth entry of the last column in the table in Figure 3. We see that in this case, γ_{T_K} contains two special components in distinct δ -gradings, since a , being the Alexander grading of a generator of $\widehat{\text{HF}}\text{K}(K)$, is an integer.
- (2) Suppose $x = x_u = y_v$ or $x = y_u = x_v$. In this case, γ_{T_K} also contains two special components in distinct δ -gradings, unless $a = 0$.

Let $K \subset S^3$ be a knot and suppose γ_{T_K} does not contain two special components in distinct δ -gradings. Then γ_K consists of a single connected component. Indeed, if there were two components, then in particular there would be a component of γ_K not containing the curve segment $\mathbf{d}_{2\tau(K)}$; a generator of maximal Alexander grading in that component would be a generator of type (1). Similarly, one can see that γ_K has the structure of the knot Floer homology of an L-space knot: All generators sit in distinct Alexander gradings and every curve segment in $S_\infty(\gamma_K)$ except $\mathbf{d}_{2\tau(K)}$ connects generators in consecutive Alexander gradings. (This is sometimes known

as the “staircase structure”.) If $\dim \widehat{\text{HFK}}(K) > 3$ this implies that there is more than one generator of type (2), and only one of them can be in Alexander grading 0. So we deduce that $\dim \widehat{\text{HFK}}(K) \leq 3$. But the only knots with such small knot Floer homology are the unknot and the two trefoil knots [OS04, Ghi08, HW18]. \square

PROOF OF PROPOSITION 1.10. Let K be as in the statement of Proposition 1.10 and suppose for contradiction that $P(K)$ is a satellite knot whose knot Floer homology is thin for some pattern P with wrapping number 2. Then $P(K) = T_P \cup T_K$ for some pattern tangle T_P and we may write

$$\widehat{\text{HFK}}(P(K)) \otimes \mathbb{F}^2 \cong \text{HF}(-\gamma_{T_P}, \gamma_{T_K}).$$

By Proposition 5.1, T_K contains two special components in distinct δ -grading. Thus, γ_{T_P} only contains component of slope ∞ , because otherwise, $\text{HF}(-\gamma_{T_P}, \gamma_{T_K})$ would not be thin by [KWZ21, Lemma 4.17]. Furthermore, by the same reasoning, using [KWZ21, Lemma 4.20], no component of γ_{T_P} can be special. So γ_{T_P} consists of rational components of slope ∞ only. By [LMZ22, Theorem 4.1], the tangle T_P is vertically split and hence the wrapping number of the pattern P is 0, contrary to our assumptions. \square

Lemma 5.2. *A knot $K \subset S^3$ is an L-space knot if and only if all special components in γ_{T_K} sit in δ -gradings of the same parity.*

PROOF. This follows from the computations in the proof of Proposition 5.1, observing the fact that generators of type (1) cannot occur. \square

PROOF OF PROPOSITION 1.11. Let P and K be as in the statement of Proposition 1.11 and suppose for contradiction that $P(K)$ is an A-link. We now argue as in the proof of Proposition 1.10, using the fact that by Lemma 5.2, γ_{T_K} contains two special components in δ -gradings of different parity. \square

PROOF OF THEOREM 1.12. By Lemma 5.2, it remains to see that there exists a non-trivial rational A-link filling of T_K if and only if all special components in γ_{T_K} sit in δ -gradings of the same parity. But this follows from [KWZ21, Lemma 4.17]. \square

It is interesting to compare the following spaces [RR17, HRW16, KWZ21]:

$$\mathcal{L}(K) := \{p/q \in \mathbb{Q}\mathbb{P}^1 \mid S_{p/q}^3(K) \text{ is an L-space}\},$$

$$\text{A}(T_K) := \{p/q \in \mathbb{Q}\mathbb{P}^1 \mid T_K(p/q) \text{ is an A-link}\}.$$

THEOREM 5.3. *For any knot $K \subset S^3$, exactly one of the following holds:*

- (1) $\mathcal{L}(K) = \{\infty\} = \text{A}(T_K)$;
- (2) $\mathcal{L}(K) = \mathbb{Q}\mathbb{P}^1 \setminus \{0\} = \text{A}(T_K)$; in this case, K is the unknot;
- (3) $\mathcal{L}(K) = [2\tau(K) - 1, \infty]$ and $\text{A}(T_K) = (4\tau(K), \infty]$; in this case, $\tau(K) > 0$;
- (4) $\mathcal{L}(K) = [\infty, 2\tau(K) + 1]$ and $\text{A}(T_K) = [\infty, 4\tau(K)]$; in this case, $\tau(K) < 0$.

PROOF. Let $K \subset S^3$ be a knot. By Theorem 1.12, $\mathcal{L}(K) = \{\infty\}$ if and only if $\text{A}(T_K) = \{\infty\}$. So it suffices to see that if K is an L-space knot, then exactly one of (2)–(4) holds. We claim that the three cases correspond precisely to the cases $\tau(K) = 0$, $\tau(K) > 0$, and $\tau(K) < 0$, respectively. Note that the unknot is the only L-space knot with $\tau(K) = 0$.

The values of $\mathcal{L}(K)$ in these three cases can be easily determined from the multicurve γ_K ; this is explained in [HRW16, Section 7.5]. So it remains to determine the value of $\text{A}(T_K)$ in these cases.

For case (2), observe that T_K is the rational tangle of slope 0, and so any rational filling of T_K is a 2-bridge link. All two-bridge links are alternating, except the unlink, which corresponds to the 0-rational filling and whose knot Floer homology is supported in two consecutive δ -gradings. So indeed $A(T_K) = \mathbb{Q}P^1 \setminus \{0\}$.

For cases (3) and (4), we first note that $A(T_K)$ contains some $p/q \neq \infty$ by Theorem 1.12. So $A(T_K)$ must be an interval [KWZ21, Theorem 1.8]. In fact, as explained in [KWZ21, Sections 2.1 and 4.2], the boundary points of the interval must be equal to ∞ and $4\tau(K)$, since γ_{T_K} is supported in these slopes. Moreover, as the curve of slope $4\tau(K)$ is rational, this slope is not contained in the interval and we already know that $\infty \in A(T_K)$. So $A(T_K)$ is either equal to $(4\tau(K), \infty]$ or $[\infty, 4\tau(K))$. We determine which one it is by observing $0 \notin A(T_K)$. This is because the determinant of the link $T_K(0) = C_{2,0}(K)$ is zero. \square

Corollary 5.4. *For any knot $K \subset S^3$ and $n \gg 0$, $S_n^3(K)$ is an L-space if and only if $C_{2,n}(K)$ is an A-link.*

PROOF. For any integer n , $T_K(n) = C_{2,n}(K)$. Now choose $n > 4|\tau(K)|$ and apply Theorem 5.3. \square

It is interesting to compare this to Hanselman and Watson's cabling formula for γ_K [HW19].

6. Growth of knot Floer and Khovanov homology under cabling

We now compare the Heegaard Floer multicurve invariant γ_T and the Khovanov multicurve invariant $\widetilde{\text{Kh}}(T; \mathbb{F}_2)$ [KWZ19] for double tangles $T = T_K$. To emphasize the similarity between the two invariants, we will in this section denote the former by γ_T^{HF} and the latter by γ_T^{Kh} . Like γ_T^{HF} , the multicurve invariant γ_T^{Kh} satisfies a gluing theorem that allows one to compute the Khovanov homology of the union of two tangles in terms of Lagrangian Floer homology [KWZ19, Theorem 1.9]. Even more remarkably, the components of γ_T^{Kh} are also subject to very similar geography restrictions [KWZ22b, Theorem 1.2]. We do not need the full statement of this classification; it suffices to say that there is a class of *rational* curves $\mathbf{r}^{\text{Kh}}(k)$, parametrized by their *slope* $k \in \mathbb{Z}$, and a class of *special* curves $\mathbf{s}_\ell^{\text{Kh}}(\infty)$, parametrized by their *length* $\ell \in 2\mathbb{Z}$. To simplify notation, we will write

$$\mathbf{s}_\ell^{\text{Kh}} := \mathbf{s}_\ell^{\text{Kh}}(\infty) \quad \text{and} \quad \mathbf{r}_k^{\text{Kh}} := \mathbf{r}^{\text{Kh}}(k).$$

For clarity, we will in this section write $\mathbf{s}_\ell^{\text{HF}}$, $\bar{\mathbf{s}}_\ell^{\text{HF}}$, and \mathbf{r}_k^{HF} for the curves previously denoted by \mathbf{s}_ℓ , $\bar{\mathbf{s}}_\ell$, and \mathbf{r}_k , respectively, for all $\ell \in \mathbb{Z}^{>0}$ and $k \in \mathbb{Z}$.

We have the following structure theorem for $\gamma_{T_K}^{\text{Kh}}$, which is implicit in [LZ22].

THEOREM 6.1. *For any knot $K \subset S^3$, the multicurve γ_{T_K} contains a single rational component $\mathbf{r}_{2\vartheta_2(K)}^{\text{Kh}}$, where $\vartheta_2(K) \in \mathbb{Z}$ is the concordance homomorphism from [LZ22], and every other curve segment is of type $\mathbf{s}_{\ell_i}^{\text{Kh}}$ for some $\ell_i > 0$.*

PROOF. The tangle T_K is the quotient tangle of a strongly invertible knot, namely $K \# r(K)$, where $r(K)$ is the reverse of K . So by [KWZ22a, Theorem 3.1], every component except one is of type $\mathbf{s}_{\ell_i}^{\text{Kh}}$ for some $\ell_i \in 2\mathbb{Z}^{>0}$, and the remaining one is of type \mathbf{r}_k^{Kh} for some slope $k \in \mathbb{Z}$. The slope k is divisible by 2 because rational components (of odd length) detect how tangle ends are connected [KWZ22b, Theorem 5.6]. (This implies that also in [KWZ22a, Theorem 3.1], the slope k is always divisible by 2.)

It remains to relate the slope k to the concordance invariant $\vartheta_2(K)$. By [LZ22, Corollary 5.14], $2\vartheta_2(K)$ is the slope of the multicurve invariant $\widehat{\text{BN}}(T_K)$ near the bottom right tangle end. By naturality of the mapping class group action on $\widehat{\text{BN}}(T_K)$ and $\widehat{\text{Kh}}(T_K)$ [KWZ19, Theorem 1.13], it suffices to show that the rational component of the twisted curve $\widehat{\text{Kh}}(T_K + Q_{-2\vartheta_2(K)})$ is 0. This follows from a simple computation carried out in [LZ22, Proof of Lemma 5.11]. \square

Remark 6.2. Combining Theorems 4.1 and 6.1, we see that the slopes of the rational components in $\gamma_{T_K}^{\text{HF}}$ and $\gamma_{T_K}^{\text{Kh}}$ are $4\tau(K)$ and $2\vartheta_2(K)$, respectively. So, as already observed in [LZ22, Section 1.3], $2\tau(K)$ plays the same role in knot Floer homology as the invariant $\vartheta_2(K)$ in Khovanov homology.

For the proofs of Propositions 1.14 and 1.15, we need the following basic result.

Lemma 6.3. *Let $k, k' \in \mathbb{Z}$ with $k \neq k'$ and $\ell \in 2\mathbb{Z}^{>0}$. Then*

$$\dim \text{HF}(\gamma, \gamma') = \begin{cases} 2\ell & \text{if } (\gamma, \gamma') \in \{(\mathbf{r}_k^{\text{Kh}}, \mathbf{s}_\ell^{\text{Kh}}), (\mathbf{r}_k^{\text{HF}}, \mathbf{s}_\ell^{\text{HF}}), (\mathbf{r}_k^{\text{HF}}, \overline{\mathbf{s}}_\ell^{\text{HF}})\} \\ 2|k' - k| & \text{if } (\gamma, \gamma') \in \{(\mathbf{r}_k^{\text{Kh}}, \mathbf{r}_{k'}^{\text{Kh}}), (\mathbf{r}_k^{\text{HF}}, \mathbf{r}_{k'}^{\text{HF}})\} \\ 4 & \text{if } \gamma = \gamma' = \mathbf{r}_k^{\text{Kh}} \\ 2 & \text{if } \gamma = \gamma' = \mathbf{r}_k^{\text{HF}} \end{cases}$$

PROOF. These are straightforward computations. \square

PROOF OF PROPOSITION 1.14. By the gluing theorem, combined with the Main Theorem,

$$\begin{aligned} 2 \dim \widehat{\text{HF\!K}}(C_{2,2t+1}(K)) &= \dim \text{HF}(\mathbf{r}_{2t+1}^{\text{HF}}, \gamma_{T_K}^{\text{HF}}) \\ &= \dim \text{HF}(\mathbf{r}_{2t+1}^{\text{HF}}, \mathbf{r}_{4\tau(K)}^{\text{HF}}) + \sum_{\mathbf{s}} \dim \text{HF}(\mathbf{r}_{2t+1}^{\text{HF}}, \mathbf{s}) \end{aligned}$$

where the sum is over all special connected components \mathbf{s} in $\gamma_{T_K}^{\text{HF}}$. The first summand is equal to $2|2t + 1 - 4\tau(K)|$ by Lemma 6.3. Each term in the second summand is equal to twice the length of the special curve \mathbf{s} . The number of terms is $(d - 1)$ by the Main Theorem, so the second term is equal to $4(d - 1)\bar{\ell}$. The desired identity follows.

The upper bound for $\dim \widehat{\text{HF\!K}}(C_{2,2t+1}(K))$ is clear. The lower bound follows from the observation that $\bar{\ell} \geq 1$ and $|2t + 1 - 4\tau(K)|$ is odd. \square

ALTERNATIVE PROOF OF PROPOSITION 1.14. We briefly outline an alternative argument that uses Hanselman and Watson's cabling formula for the multicurve invariant γ_K [HW19]. As noted in the introduction, for any knot $K \subset S^3$, the dimension of $\widehat{\text{HF\!K}}(K)$ is equal to the minimal number of intersection points of γ_K with the meridian μ_K (counted with multiplicity of the dimension of any local system). Equivalently, $\dim \widehat{\text{HF\!K}}(K)$ is equal to the number of elements in $S_{\infty}(\gamma_K)$. The same is true, of course, if we replace K by $K' := C_{2,2t+1}(K)$. Using Hanselman and Watson's cabling formula, we can easily compute the multicurve $\gamma_{K'}$ from γ_K ; in particular, we determine $S_{\infty}(\gamma_{K'})$ from $S_{\infty}(\gamma_K)$ as follows: Every component \mathbf{u}_ℓ contributes a single component $\mathbf{u}_{\ell'}$ (for some $\ell' \in \mathbb{Z}^{>0}$), ℓ components \mathbf{u}_1 and $(\ell - 1)$ components \mathbf{v}_1 in $S_{\infty}(\gamma_{K'})$. Similarly, \mathbf{v}_ℓ contributes a total of 2ℓ components in $S_{\infty}(\gamma_{K'})$. From this, we get the first summand in Proposition 1.14. The second summand comes from the contribution of $\mathbf{d}_{2\tau(K)}$. This curve contributes a single

component $\mathbf{d}_{2\tau(K')}$ to $S_{\infty}(\gamma_{K'})$ as well as $\lfloor \frac{2t+1}{2} - 2\tau(K) \rfloor$ pairs of components \mathbf{u}_1 and \mathbf{v}_1 . \square

PROOF OF PROPOSITION 1.15. We start by observing that each of the two components of the link $C_{2,2t}(K)$ is equal to K . So by [BS15, Corollary 1.6],

$$\dim \text{Kh}(C_{2,2t}(K)) \geq (\dim \text{Kh}(K))^2,$$

where $\text{Kh}(\cdot)$ denotes unreduced Khovanov homology over \mathbb{F}_2 . Thus, for reduced Khovanov homology $\widetilde{\text{Kh}}(\cdot)$, we obtain

$$(6.1) \quad \dim \widetilde{\text{Kh}}(C_{2,2t}(K)) \geq 2(\dim \widetilde{\text{Kh}}(K))^2 = 2d^2,$$

since $\dim \text{Kh}(J) = 2 \dim \widetilde{\text{Kh}}(J)$ for any link J [Shu04, Corollary 3.2.C]. By the gluing theorem, combined with Theorem 6.1,

$$\begin{aligned} 2 \dim \widetilde{\text{Kh}}(C_{2,k}(K)) &= \dim \text{HF}(\mathbf{r}_k^{\text{Kh}}, \gamma_{T_K}^{\text{Kh}}) \\ &= \dim \text{HF}(\mathbf{r}_k^{\text{Kh}}, \mathbf{r}_{2\vartheta_2(K)}^{\text{Kh}}) + \sum_{\mathbf{s}} \dim \text{HF}(\mathbf{r}_k^{\text{Kh}}, \mathbf{s}) \end{aligned}$$

for any integer k , where the sum is over all special components \mathbf{s} in $\gamma_{T_K}^{\text{Kh}}$. The first summand is equal to $2|k - 2\vartheta_2(K)|$, unless $k = 2\vartheta_2(K)$, in which case it is equal to 4. The second summand is independent of k . Setting $k = 2t + 1$ and $k = 2\vartheta_2(K)$, we obtain

$$\dim \widetilde{\text{Kh}}(C_{2,2t+1}(K)) = \dim \widetilde{\text{Kh}}(C_{2,2\vartheta_2(K)}(K)) - 2 + |2t + 1 - 2\vartheta_2(K)|$$

We now combine this identity with (6.1) and obtain the desired inequality. \square

I close with a few remarks about Conjecture 1.16. I have verified this conjecture for a selection of about 30 knots with up to 11 crossings using the computer program [Zib21]. The conjecture is also consistent with Proposition 1.15—at least, if we assume the following conjecture, which generalises [KWZ22a, Conjecture 3.10] and for which there is now overwhelming computational evidence.

Conjecture 6.4. *For any Conway tangle T , the length of every special component of $\gamma_T^{\text{Kh}} = \widetilde{\text{Kh}}(T; \mathbb{F}_2)$ is divisible by 4.*

Note this conjecture is known to be false if $\widetilde{\text{Kh}}(T; \mathbb{F}_2)$ is computed over a field of different characteristic. Now, assuming Conjectures 1.16 and 6.4, Proposition 1.15 follows by the same argument as Proposition 1.14. By the gluing theorem,

$$\begin{aligned} 2 \dim \widetilde{\text{Kh}}(C_{2,2t+1}(K)) &= \dim \text{HF}(\mathbf{r}_{2t+1}^{\text{Kh}}, \gamma_{T_K}^{\text{Kh}}) \\ &= \dim \text{HF}(\mathbf{r}_{2t+1}^{\text{Kh}}, \mathbf{r}_{2\vartheta_2(K)}^{\text{Kh}}) + \sum_{\mathbf{s}} \dim \text{HF}(\mathbf{r}_{2t+1}^{\text{Kh}}, \mathbf{s}), \end{aligned}$$

where the sum is over all special connected components \mathbf{s} in $\gamma_{T_K}^{\text{Kh}}$. By assumption, there are at least $\frac{1}{2}(d^2 - 1)$ such components (where $d = \dim \widetilde{\text{Kh}}(K)$) and each of them contributes at least 8 to the expression above. So the overall contribution of special components of $\gamma_{T_K}^{\text{Kh}}$ to $\dim \widetilde{\text{Kh}}(C_{2,2t+1}(K))$ is $2(d^2 - 1)$, i.e. the first two summands in Proposition 1.15. The remaining summand is equal to the contribution of the rational component of $\gamma_{T_K}^{\text{Kh}}$.

References

- [BGH21] Steven Boyer, Cameron McA Gordon, and Ying Hu, *Slope detection and toroidal 3-manifolds*, 2021, [arXiv:2106.14378](#).
- [BS15] Joshua Batson and Cotton Seed, *A link-splitting spectral sequence in Khovanov homology*, *Duke Mathematical Journal* **164** (2015), no. 5, 801–841, [arXiv:1303.6240](#).
- [Dey19] Subhankar Dey, *Cable knots are not thin*, 2019, [arXiv:1904.11591](#).
- [Ghi08] Paolo Ghiggini, *Knot Floer homology detects genus-one fibred knots*, *Amer. J. Math.* **130** (2008), no. 5, 1151–1169, [arXiv:math/0603445](#).
- [Han19] Jonathan Hanselman, *github repository for immersed curve invariants of knot complements*, 2019, <https://github.com/hanselman/CFK-immersed-curves/>.
- [HRW16] Jonathan Hanselman, Jacob Rasmussen, and Liam Watson, *Bordered Floer homology for manifolds with torus boundary via immersed curves*, 2016, [arXiv:1604.03466](#).
- [HRW22] ———, *Heegaard Floer homology for manifolds with torus boundary: properties and examples*, *Proc. Lond. Math. Soc.* **125** (2022), no. 4, 879–967, [arXiv:1810.10355](#).
- [HW15] Jonathan Hanselman and Liam Watson, *A calculus for bordered Floer homology*, 2015, [arXiv:1508.05445](#), to appear in *Geom. Topol.*
- [HW18] Matthew Hedden and Liam Watson, *On the geography and botany of knot Floer homology*, *Selecta Math. (N.S.)* **24** (2018), no. 2, 997–1037, [arXiv:1404.6913](#).
- [HW19] Jonathan Hanselman and Liam Watson, *Cabling in terms of immersed curves*, 2019, [arXiv:1908.04397](#), to appear in *Geom. Topol.*
- [KWZ19] Artem Kotelskiy, Liam Watson, and Claudius Zibrowius, *Immersed curves in Khovanov homology*, 2019, [arXiv:1910.14584](#).
- [KWZ20] ———, *A mnemonic for the Lipshitz-Ozsváth-Thurston correspondence*, 2020, [arXiv:2005.02792](#), to appear in *Algebr. Geom. Topol.*
- [KWZ21] ———, *Thin links and Conway spheres*, 2021, [arXiv:2105.06308](#).
- [KWZ22a] ———, *Khovanov homology and strong inversions*, *Open Book Series* **5** (2022), no. 1, 223–244, [arXiv:2104.13592](#).
- [KWZ22b] ———, *Khovanov multicurves are linear*, 2022, [arXiv:2202.01460](#).
- [LMZ22] Tye Lidman, Allison H. Moore, and Claudius Zibrowius, *L-space knots have no essential Conway spheres*, *Geom. Topol.* **26** (2022), no. 5, 2065–2102, [arXiv:2006.03521](#).
- [LOT18] Robert Lipshitz, Peter S. Ozsváth, and Dylan P. Thurston, *Bordered Heegaard Floer homology*, *Mem. Amer. Math. Soc.* **254** (2018), no. 1216, viii+279, [arXiv:0810.0687v5](#).
- [LZ22] Lukas Lewark and Claudius Zibrowius, *Rasmussen invariants of Whitehead doubles and other satellites*, 2022, [arXiv:2208.13612](#).
- [OS04] Peter Ozsvath and Zoltan Szabo, *Holomorphic disks and genus bounds*, *Geometry & Topology* **8** (2004), no. 1, 311–334, [arXiv:math/0311496](#).
- [OS05a] P. Ozsváth and Z. Szabó, *On knot Floer homology and lens space surgeries*, *Topology* **44** (2005), no. 6, 1281–1300, [arXiv:math/0303017](#). MR 2168576
- [OS05b] Peter Ozsváth and Zoltán Szabó, *On the Heegaard Floer homology of branched double-covers*, *Advances in Mathematics* **194** (2005), no. 1, 1–33, [arXiv:math/0309170](#).
- [OS17] ———, *Knot Floer homology calculator*, <https://web.math.princeton.edu/~szabo/HFKcalc.html>, 2017.
- [OSS15] Peter S. Ozsváth, András I. Stipsicz, and Zoltán Szabó, *Grid homology for knots and links*, vol. 208, *Math. Surv. Monogr.*, Am. Math. Soc., 2015.
- [PW21] Ina Petkova and Biji Wong, *Twisted Mazur pattern satellite knots and bordered Floer theory*, 2021, [arXiv:2005.12795](#).
- [RR17] Jacob Rasmussen and Sarah Dean Rasmussen, *Floer simple manifolds and L-space intervals*, *Adv. Math.* **322** (2017), 738–805. MR 3720808
- [Shu04] Alexander N. Shumakovitch, *Torsion of the Khovanov homology*, *Fund. Math.* (2004), 343–364, [arXiv:math/0405474](#).
- [Zar11] Rumen Zarev, *Bordered sutured Floer homology*, ProQuest LLC, Ann Arbor, MI, 2011, Thesis (Ph.D.)—Columbia University. (doi: 10.7916/D83R10V4).
- [Zib18] Claudius Zibrowius, *PQM.m*, 2018, Mathematica package for computing the Heegaard Floer multicurve invariant for Conway tangles, available from the author’s website.
- [Zib19a] ———, *Kauffman states and Heegaard diagrams for tangles*, *Algebr. Geom. Topol.* **19** (2019), no. 5, 2233–2282, [arXiv:1601.04915](#).

- [Zib19b] ———, *On symmetries of peculiar modules; or, δ -graded link Floer homology is mutation invariant*, 2019, [arXiv:1909.04267v2](https://arxiv.org/abs/1909.04267v2), to appear in J. Eur. Math. Soc.
- [Zib20] ———, *Peculiar modules for 4-ended tangles*, J. Topol. **13** (2020), no. 1, 77–158, [arXiv:1712.05050v3](https://arxiv.org/abs/1712.05050v3).
- [Zib21] ———, *kht++*, a program for computing Khovanov invariants for links and tangles, <https://cbz20.raspberrypi.com/code/khttp/docs/>, 2021.
- [Zib22] ———, *python script domains.py*, ancillary file to this article, 2022, available at <https://cbz20.raspberrypi.com/code/ancillary/HF2HFT/domains.py>.
- [Zib23] ———, *python script hf2hft.py*, ancillary file to this article, 2023, available at <https://cbz20.raspberrypi.com/code/ancillary/HF2HFT/hf2hft.py>.

DURHAM UNIVERSITY, DEPARTMENT OF MATHEMATICAL SCIENCES, UNITED KINGDOM

Email address: cbz20@posteo.net

URL: <https://cbz20.raspberrypi.com/>